

Three-dimensional AdS black holes in massive-power-Maxwell theory

B. Eslam Panah^{1,2,3*}, Kh. Jafarzade^{1,2†}, A. Rincón^{4‡}

¹ *Department of Theoretical Physics, Faculty of Basic Sciences,
University of Mazandaran, P. O. Box 47416-95447, Babolsar, Iran*

² *ICRANet-Mazandaran, University of Mazandaran, P. O. Box 47416-95447, Babolsar, Iran*

³ *ICRANet, Piazza della Repubblica 10, I-65122 Pescara, Italy*

⁴ *Sede Esmeralda, Universidad de Tarapacá, Avda. Luis Emilio Recabarren 2477, Iquique, Chile*

Recently, it was shown that power-Maxwell (PM) theory can remove the singularity of electric field [1]. Motivated by great interest in three-dimensional black holes and a surge of success in studying massive gravity from both the cosmological and astrophysical point of view, we investigate such black hole solutions in de Rham, Gabadadze and Tolley (dRGT) massive theory of gravity in the presence of PM electrodynamics. First, we extract exact three-dimensional solutions in the PM-dRGT massive gravity. Then we study geometrical properties including type of singularity and asymptotic behavior, and show that although there is a singularity at the origin for asymptotical (A)dS, only AdS solutions are covered by an event horizon. Calculating conserved and thermodynamic quantities, we check the validity of the first law of thermodynamics for the corresponding solutions and examine the stability of these black holes in context of canonical ensemble. We continue with the calculation of the optical features of this kind of black holes such as the shadow geometrical shape, the energy emission rate and the deflection angle. Taking into account these optical quantities, we analysis the effective role of the parameters of models on them. We also employ the correspondence between the quasinormal modes in the eikonal limit and shadow radius to study the scalar field perturbations in these backgrounds. Finally, we take advantage of the WKB method and investigate how the quasinormal modes will be disturbed for massive particles.

I. INTRODUCTION

Considering General Relativity (GR) in three-dimensional spacetime, Banados, Teitelboim and Zanelli (BTZ) have found black hole solutions [2], which are known as BTZ Black holes. The study of BTZ black holes opened different aspects of physics in three-dimensional spacetime such as the existence of specific relations between the BTZ black holes and effective action in string theory [3–5], providing simplified machinery for studying different features of black holes such as thermodynamic ones [6–11], contributing to our understanding of gravitational systems and their interactions in lower dimensions [12], possible existence of gravitational Aharonov-Bohm effect due to the non-commutative BTZ black holes [13], AdS/CFT correspondence [14, 15], quantum aspect of three-dimensional gravity, entanglement and quantum entropy [16–21], holographic aspects of BTZ black hole solutions [22–24], anti-Hawking phenomena of BTZ black holes [25, 26]. Also, the BTZ black hole is currently a seminal toy model to study different effects beyond GR. In particular, it is well known that quantum features can be systematically included if we relax certain facts assumed in the GR. Thus, in the context of quantum theories of gravity, we have several examples where the coupling constant which parameterize the theory can be treated a function which evolve in spacetime to account the corresponding quantum features. Such is the case, for instance of scale dependent gravity: a simple theory based on asymptotically safe gravity implemented to study different physics effects. As has been reported before, in theories of gravity, the scale dependence is expected to modify the horizon, the thermodynamics as well as the quasinormal spectra of classical black hole backgrounds [27–35]. What is more, the Sagnac effect [36], the evolution of trajectories of photons [37], some cosmological solutions [38], and transverse wormhole solutions [39] have also been studied too. A closed related approach is usually called improvement asymptotically safe gravity [40–42]. Also, for RG-improved cosmologies and inflationary models from asymptotic safety see e.g. [43–46], and for recent progress [47–50]. On the other hand, by considering various theories of gravity coupled with different matter fields, three-dimensional black hole solutions and their thermodynamic properties have been studied in literature [51–61]. In the present work, motivated by interesting properties of three-dimensional black hole solutions, we will conduct our study in this dimension of spacetime.

One of the most challenging problems of modern cosmology is related to the fact that our Universe is expanding with acceleration. Some candidates have been proposed to explain this acceleration such as the existence of a positive cosmological constant [62, 63], dark energy [64–66], and modified theories of gravity [67–72].

* email address: eslampanah@umz.ac.ir

† email address: khadije.jafarzade@gmail.com

‡ email address: aerinconr@academicos.uta.cl

Among different candidates of modified theories of gravity, massive theories of gravity have attracted a lot of attentions lately due to a wide variety of motivations in various aspects of physics [73, 74]. From a cosmological point of view, one can point out to interesting features such as describing the accelerating expansion of our Universe without requiring any dark energy [75, 76], explaining the current observations related to dark matter [77, 78], suitable description of rotation curves of the Milky Way, spiral galaxies, and low surface brightness galaxies [79]. The most important achievements in the astrophysics context are: the existence of white dwarfs more than the Chandrasekhar limit [80], and massive neutron stars with maximum mass more than three times the solar mass [81]. To name a few in the point of black hole physics, one can mention: the existence of van der Waals like behavior in extended phase space for non-spherical black holes [82, 83], triple points and N-fold reentrant phase transitions [84], the existence of a remnant for a black hole which may help to ameliorate the information paradox [85, 86], etc.

In recent years, a new version of theory of massive gravity is proposed by de Rham, Gabadadze and Tolley (dRGT) [87, 88], which is known as dRGT massive gravity. The dRGT massive gravity's action contains a nonlinear interaction term which admits the Vainshtein mechanism and is free from van Dam-Veltman-Zakharov discontinuity [89, 90], and Boulware-Deser ghost [91, 92], in arbitrarily dimensions (which appears in Fierz-Pauli theory of massive gravity [93]). It is notable that the dRGT theory of massive gravity requires a fiducial reference metric ($f_{\mu\nu}$) in addition to the dynamical metric ($g_{\mu\nu}$) in order to define a mass term for graviton by introducing some non-derivative potential terms (\mathcal{U}_i). Also, modification in the introduced reference metric leads to a special family of dRGT massive gravity [74]. So, different reference metrics could lead to a variety of new solutions. In this regards, it was shown that the dRGT massive gravity is ghost-free by considering different reference metrics such as Minkowski and degenerate (singular) reference metrics (see Refs. [94–96], for more details). Asymptotically flat and (A)dS black holes in the context of massive gravity have been obtained by considering the flat (Minkowski) reference metric or on a degenerate (spatial) and singular reference metric [97–102].

One of interesting cases of theories of massive gravity is related to the AdS black hole solutions with the degenerate (spatial) reference metric which is singular and has important applications in gauge/gravity duality (see Ref. [102], for more details). In this theory of massive gravity, graviton may behave like a lattice and exhibits a Drude peak [102]. It was indicated that this theory of massive gravity is stable and ghost-free [95]. Black hole solutions in the context of this massive gravity have been studied in Refs. [103, 104]. Study on black holes in this theory has attracted extensive attention recently, ranging from heat engine and Joule-Thomson expansion [105, 106], quasinormal modes [107, 108], van der Waals-like phase transition [82–84, 105, 109], reentrant phase transitions and triple points [110], phase transition and entropic force [111], thermodynamics and geometrical thermodynamics [112–116], correspondence between black hole solutions of conformal and massive theories of gravity [117].

Another fascinating subject which has gained significant attention is related to coupling of theories of gravity with nonlinear electrodynamics (NED). The power-Maxwell (PM) theory is one of the interesting and special classes of NED which was presented by Hassaine and Martinez in 2007 [118]. Recently, it was shown that PM theory similar to Born-Infeld theory can remove the singularity of electric field at the origin [1]. Lagrangian of PM theory is an arbitrary power of Maxwell Lagrangian, where it is invariant under the conformal transformation $g_{\mu\nu} \rightarrow \Omega^2 g_{\mu\nu}$ (where $g_{\mu\nu}$ is metric tensor) and $A_\mu \rightarrow A_\mu$, see Refs. [119, 120], for more details. It is worthwhile to mention that the PM theory reduces to linear Maxwell theory when the power of Maxwell is unit [119, 120]. Another marvelous feature of PM is related to its conformal invariancy. As we know, the Maxwell action enjoys conformal invariance in four-dimensions, but in higher dimensions, it does not possess this symmetry. However, the Lagrangian of PM theory extends the conformal invariance in higher dimensions if the power is chosen as $s = (\text{dimensions of spacetime})/4$ (where s is power of PM theory). This leads to black hole solutions which are inverse square electric field in arbitrary dimensions (the so-called Coulomb law). In this regards, some interesting properties of black hole solutions coupled to the PM theory have been studied in Refs. [121–127]. Generalization of GR with a massive spin-2 field Lagrangian minimally coupled to a PM $U(1)$ gauge field in four and higher dimensional spacetime have been investigated in Refs. [84, 128], which led to some novel and interesting properties in black hole physics.

Taking into account the mentioned motivations, in this paper we are going to extract three-dimensional black hole solutions by considering three generalizations, a massive spin-2 field, a PM $U(1)$ gauge field and the cosmological constant to the Einstein-Hilbert Lagrangian. Then we study the properties of them from various perspective.

II. BASIC EQUATIONS

The three-dimensional action of Einstein-dRGT massive gravity coupled with the PM nonlinear electrodynamics is given by [128]

$$\mathcal{I} = -\frac{1}{16\pi} \int d^3x \sqrt{-g} [\mathcal{R} - 2\Lambda + (-\mathcal{F})^s + m_g^2 \varepsilon \mathcal{U}(g, f)], \quad (1)$$

where R , and Λ are the scalar curvature and the cosmological constant, respectively. Also $\mathcal{F} = F_{\mu\nu}F^{\mu\nu}$ is the Maxwell invariant (where $F_{\mu\nu} = \partial_\mu A_\nu - \partial_\nu A_\mu$ and A_μ are the Faraday tensor and the gauge potential, respectively). Here, s is related to power of PM theory. It is straightforward to show that the term $(-\mathcal{F})^s$ reduces to the standard Maxwell Lagrangian for $s = 1$. In the above action, m_g and f are related to the graviton mass and a fixed symmetric tensor, respectively. Note that ε is a constant and also \mathcal{U} is a self-interaction potential of graviton constructed from the building blocks $\mathcal{K}_\nu^\mu = \sqrt{g^{\mu\alpha}f_{\alpha\nu}}$, in which for the three-dimensional spacetime \mathcal{U} is in the following form

$$\mathcal{U}(g, f) = [\mathcal{K}],$$

Taking into account the action (1) and using the variational principle, we can extract the field equations related to the gravitation and gauge fields as [128]

$$G_{\mu\nu} + \Lambda g_{\mu\nu} + m_g^2 \chi_{\mu\nu} = \frac{1}{2} g_{\mu\nu} (-\mathcal{F})^s + 2s (-\mathcal{F})^{s-1} F_{\mu\rho} F_\nu^\rho, \quad (2)$$

$$\partial_\mu \left(\sqrt{-g} (-\mathcal{F})^{s-1} F^{\mu\nu} \right) = 0, \quad (3)$$

where $G_{\mu\nu} = R_{\mu\nu} - \frac{1}{2} g_{\mu\nu} R$, is Einstein's tensor. Also $\chi_{\mu\nu}$ is the massive term with the following form

$$\chi_{\mu\nu} = -\frac{\varepsilon}{2} (\mathcal{U} g_{\mu\nu} - \mathcal{K}_{\mu\nu}). \quad (4)$$

III. BLACK HOLE SOLUTIONS

In this section, we are interested in studying the three-dimensional static black holes with (a)dS asymptotic in the presence of PM theory and Einstein-dRGT-massive gravity. In this regards, we consider the metric of three-dimensional static spacetime with following explicit form

$$ds^2 = -g(r)dt^2 + g^{-1}(r)dr^2 + r^2 d\varphi^2, \quad (5)$$

where $g(r)$ is an arbitrary function of radial coordinate.

In order to obtain exact solutions, we should make a choice for the reference metric. We consider the following ansatz metric [129]

$$f_{\mu\nu} = \text{diag}(0, 0, c^2), \quad (6)$$

where c is a positive constant. Using the metric ansatz (6), \mathcal{U} is given by [129]

$$\mathcal{U} = \frac{c}{r}. \quad (7)$$

Due to the fact that we are going to study the electrically charged black holes, we consider a radial electric field which its related gauge potential is

$$A_\mu = h(r) \delta_\mu^t. \quad (8)$$

Using the metric (Eq. (5)) and the PM field equation (Eq. (3)), one finds the following differential equation

$$r h''(r) + \Psi_1 = 0, \quad (9)$$

where

$$\Psi_1 = \begin{cases} h'(r) & s = 1 \\ 2h'(r) & s = \frac{3}{4} \\ -h'(r) - 2srh''(r) & \text{otherwise} \end{cases}, \quad (10)$$

where the prime and double prime are the first and the second derivatives versus r , respectively. It is easy to find the solution of Eq. (10) as

$$h(r) = \begin{cases} \frac{q}{l} \ln\left(\frac{r}{l}\right) & s = 1 \\ \frac{-q^{2/3}}{r} & s = \frac{3}{4} \\ \frac{(2s-1)(qr^{-2s})^{\frac{1-s}{s(2s-1)}}}{2(s-1)} & \text{otherwise} \end{cases}, \quad (11)$$

where q is an integration constant which is related to the electric charge and l is an arbitrary constant with length dimension which is coming from the fact that the logarithmic arguments should be dimensionless.

It is notable that the electromagnetic field tensor is given by

$$F_{tr} = E(r) = \begin{cases} \frac{q}{lr} & s = 1 \\ \frac{q^{2/3}}{r^2} & s = \frac{3}{4} \\ \left(qr^{\frac{-s}{1-s}}\right)^{\frac{1-s}{s(2s-1)}} & \text{otherwise} \end{cases}. \quad (12)$$

Worth mentioning that the electromagnetic gauge potential (Eq. (11)) and the electromagnetic field (Eq. (12)), should be finite at infinity. These constraints impose following restriction on the nonlinearity parameter (s) as

$$\frac{1}{2} < s \leq 1. \quad (13)$$

Now, we would like to obtain exact solutions for the metric function $f(r)$. For this purpose, by employing Eqs (2) and (5), we obtain the following differential equations

$$eq_{tt} = eq_{rr} = rg'(r) + 2\Lambda r^2 - m_g^2 c\epsilon r + 2^s (2s-1) \Psi_2 = 0, \quad (14)$$

$$eq_{\varphi\varphi} = \frac{r^2 g''(r)}{2} + \Lambda r^2 - 2^{s-1} \Psi_2 = 0, \quad (15)$$

where Ψ_2 is

$$\Psi_2 = \begin{cases} \frac{q^2}{l^2} & s = 1 \\ \frac{q}{r} & s = \frac{3}{4} \\ \left(\frac{q}{r}\right)^{\frac{2(1-s)}{2s-1}} & \text{otherwise} \end{cases}, \quad (16)$$

which eq_{tt} , eq_{rr} and $eq_{\varphi\varphi}$ are corresponding to tt , rr and $\varphi\varphi$ components of Eq. (2), respectively. After some manipulations, one can obtain the following metric function

$$g(r) = -m_0 - \Lambda r^2 + m_g^2 c\epsilon r + \begin{cases} \frac{-2q^2}{l^2} \ln\left(\frac{r}{l}\right) & s = 1 \\ \frac{q}{2^{1/4} r} & s = \frac{3}{4} \\ \frac{2^{s-1}(2s-1)^2 \left(\frac{q}{r}\right)^{\frac{2(1-s)}{2s-1}}}{(1-s)} & \text{otherwise} \end{cases}, \quad (17)$$

where m_0 is an integration constant which is related to the total mass of the black hole. We should note that the obtained metric function satisfies all components of the field equation (2), simultaneously.

In order to examine the geometrical structure of these solutions, first we look for essential singularity(ies) by

calculation of the Ricci and Kretschmann scalars. We obtain exact these scalars in the following forms

$$R = 6\Lambda - \frac{2m_g^2 c \varepsilon}{r} + \begin{cases} \frac{2q^2}{l^2 r^2} & s = 1 \\ 0 & s = \frac{3}{4} \\ \frac{2^s (4s-3)}{r^2} \left(\frac{q}{r}\right)^{\frac{2(1-s)}{2s-1}} & \text{otherwise} \end{cases}, \quad (18)$$

$$R_{\alpha\beta\gamma\delta} R^{\alpha\beta\gamma\delta} = 12\Lambda^2 - \frac{8\Lambda m_g^2 c \varepsilon}{r} + \frac{2m_g^4 c^2 \varepsilon^2}{r^2} + \begin{cases} \frac{8\Lambda q^2}{l^2 r^2} - \frac{8q^2 m_g^2 c \varepsilon}{l^2 r^3} + \frac{12q^4}{l^4 r^4} & s = 1 \\ -\frac{2^{7/4} q m_g^2 c \varepsilon}{r^4} + \frac{3\sqrt{2} q^2}{r^6} & s = \frac{3}{4} \\ \frac{2^{s+2} \left(\frac{q}{r}\right)^{\frac{4(1-s)}{2s-1}}}{r^4} \left(\frac{\Lambda(4s-3)r^2 - (2s-1)m_g^2 c \varepsilon r}{\left(\frac{q}{r}\right)^{\frac{2(1-s)}{2s-1}}} + 2^{s+1} \left(s^2 - s + \frac{3}{8}\right) \right) & \text{otherwise} \end{cases}. \quad (19)$$

It is evident that the Ricci and Kretschmann scalars diverge at the origin as

$$\lim_{r \rightarrow 0} R = \infty, \quad (20)$$

$$\lim_{r \rightarrow 0} R_{\alpha\beta\gamma\delta} R^{\alpha\beta\gamma\delta} = \infty,$$

so, there is a curvature singularity at $r = 0$.

Also, for large values of radial coordinate, $r \rightarrow \infty$, the Ricci and Kretschmann scalars are

$$\lim_{r \rightarrow \infty} R = 6\Lambda, \quad (21)$$

$$\lim_{r \rightarrow \infty} R_{\alpha\beta\gamma\delta} R^{\alpha\beta\gamma\delta} = 12\Lambda^2,$$

in which confirm that the asymptotical behavior of the solution is dS for $\Lambda > 0$ and adS for $\Lambda < 0$.

In order to study the effects of massive gravitons (m_g), parameter of PM theory (s), electrical charge (q) and the cosmological constant (Λ), one can investigate the metric function (Eq. (17)). Regarding various terms of $g(r)$, it is worthwhile to mention that q -term (the fourth term in Eq. (17)) is dominant near the origin ($r \rightarrow 0$). Therefore one can conclude that the singularity is timelike. In addition, for large distance ($r \rightarrow \infty$), Λ -term (the second term in Eq. (17)) is dominant which confirms that the solutions can be asymptotically (a)dS. As one can see, the behavior of $g(r)$ is highly sensitive to the massive graviton, the parameter of PM theory, the electrical charge and the cosmological constant (see Fig. 1, for more details). It is evident that for specific values of different parameters, the metric function could have two roots, one extreme root or no root (see up panels in Fig. 1). Since any black hole has to be covered by an event horizon, our findings confirm that the (un)charged three-dimensional dS solution cannot be black hole solution (see the down panels in Fig. 1). The event horizon is defined as outer root of metric function when its slope is positive (i.e. $g'(r)|_{r=r_+} > 0$). On the other hand, the three-dimensional solutions are covered by an event horizon for $\Lambda < 0$, which confirms the existence of AdS black hole solutions in the three-dimensional spacetime.

IV. THERMODYNAMICS

Now, we intend to calculate the conserved and thermodynamic quantities of these black hole solutions and examine the validity of the first law of thermodynamics.

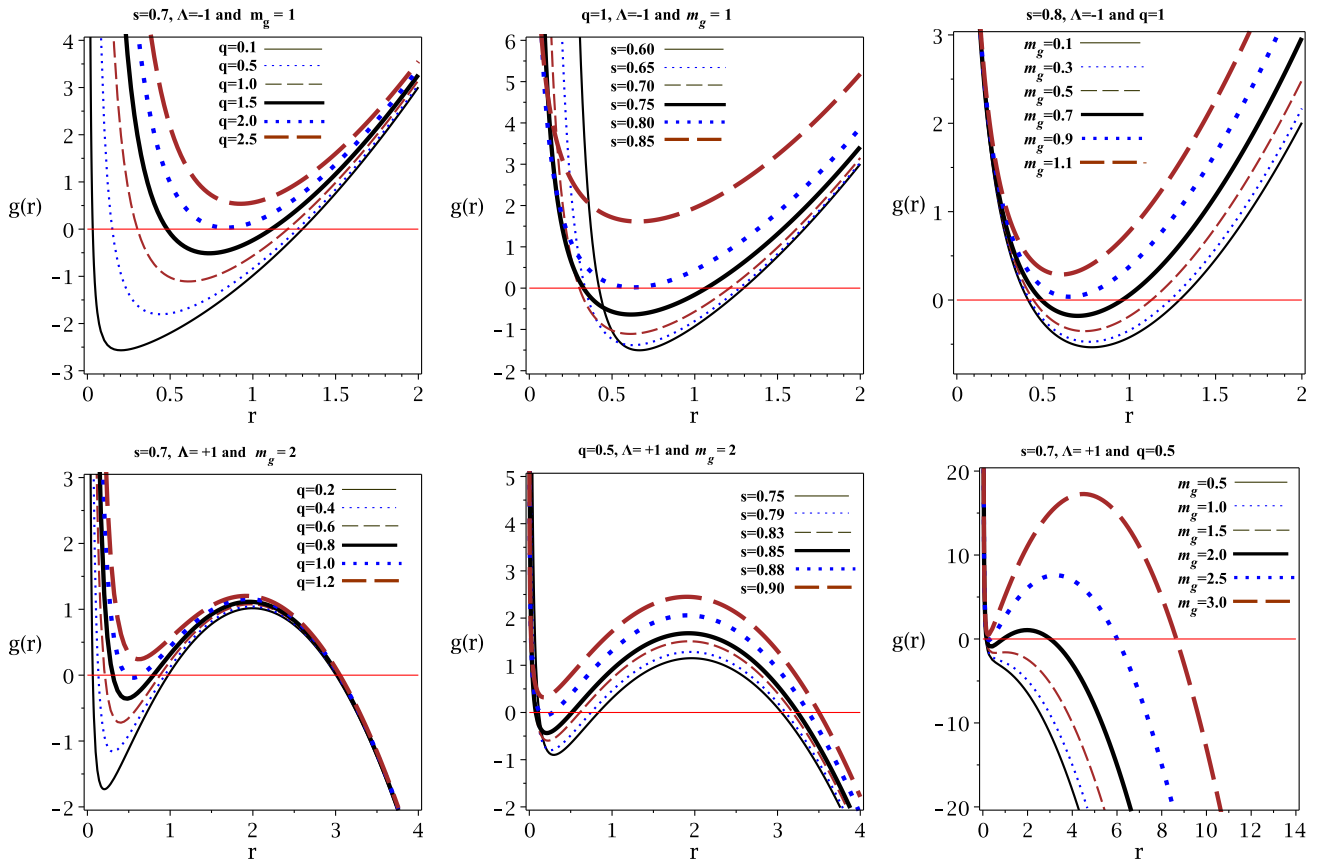


FIG. 1: $g(r)$ versus r for $\varepsilon = 1$, $c = 1$ and $m_0 = 3$. Up panels for negative value of the cosmological constant ($\Lambda = -1$). Down panels for positive value of the cosmological constant ($\Lambda = +1$).

Using the definition of Hawking temperature associated to the surface gravity on the outer horizon r_+ , one can find

$$T = -\frac{\Lambda r_+}{2\pi} + \frac{m_g^2 c \varepsilon}{4\pi} - \begin{cases} \frac{q^2}{2\pi l^2 r_+} & s = 1 \\ \frac{q}{2^{9/4} \pi r_+^2} & s = \frac{3}{4} \\ \frac{2^{s-2} (2s-1)}{\pi r_+} \left(\frac{q}{r_+} \right)^{\frac{2(1-s)}{2s-1}} & \text{otherwise} \end{cases} . \quad (22)$$

According to the Gauss's law, the electric charge, Q , can be found by calculating the flux of the electric field at infinity, yielding

$$Q = \begin{cases} \frac{q}{2l} & s = 1 \\ \frac{3q^{1/3}}{2^{13/4}} & s = \frac{3}{4} \\ 2^{s-2} s q^{\frac{1-s}{s}} & \text{otherwise} \end{cases} . \quad (23)$$

Employing the Hamiltonian approach and/or the counterterm method, one can find the total mass of the solutions as

$$M = \frac{m_0}{8}, \quad (24)$$

in which by evaluating metric function on the horizon ($f(r = r_+) = 0$), we obtain

$$M = \frac{-\Lambda r_+^2 + m_g^2 c \epsilon r_+}{8} + \begin{cases} -\frac{q^2 \ln\left(\frac{r_+}{l}\right)}{4l^2} & s = 1 \\ \frac{q}{2^{13/4} r_+} & s = \frac{3}{4} \\ \frac{2^{s-4} (2s-1)^2 \left(\frac{q}{r_+}\right)^{\frac{2(1-s)}{2s-1}}}{(1-s)} & \text{otherwise} \end{cases} .$$

For black holes in the presence of Einstein-massive gravity, the area law proposed by Hawking and Bekenstein is a valid method for calculating entropy. It is a matter of calculation to show that entropy has the following form [130–133]

$$S = \frac{\pi}{2} r_+ . \quad (25)$$

The electric potential, U , is defined through the gauge potential in the following form

$$U = A_\mu \chi^\mu |_{r \rightarrow \text{reference}} - A_\mu \chi^\mu |_{r \rightarrow r_+} = \begin{cases} -\frac{q}{l} \ln\left(\frac{r_+}{l}\right) & s = 1 \\ \frac{q^{2/3}}{r_+} & s = \frac{3}{4} \\ \frac{(2s-1) \left(q r_+^{-2s}\right)^{\frac{1-s}{s(2s-1)}}}{2(1-s)} & \text{otherwise} \end{cases} , \quad (26)$$

Having conserved and thermodynamic quantities at hand, we are in a position to check the validity of the first law of thermodynamics. It is easy to show that by using thermodynamic quantities such as electric charge (23), entropy (25) and mass (24), with the first law of black hole thermodynamics

$$dM = T dS + U dQ, \quad (27)$$

one can define the intensive parameters conjugate to S and Q . These quantities are the temperature and the electric potential

$$T = \left(\frac{\partial M}{\partial S}\right)_Q \quad \& \quad U = \left(\frac{\partial M}{\partial Q}\right)_S, \quad (28)$$

which are the same as those calculated for the temperature (22) and the electric potential (26). In other word, although massive term modifies some of thermodynamic quantities, the first law of thermodynamics is still valid.

A. Thermal stability in the canonical ensemble

Here, we study thermal stability criteria and the effects of different parameters on them. The stability conditions in canonical ensemble are based on the sign of the heat capacity. This change of sign could happen when heat capacity meets root(s) or divergency(ies). The root of heat capacity (or temperature) indicates a bound point, which separates physical solutions (positive temperature) from non-physical ones (negative temperature). Whereas heat capacity divergencies (the roots of denominator of heat capacity) represent phase transition points. The negativity of heat capacity represents unstable solutions which may undergo a phase transition and acquire stable state. In order to get a better picture and enrich the results of our study, we investigate both temperature and heat capacity, simultaneously.

The heat capacity is given by the following traditional relation

$$C_Q = \frac{T}{\left(\frac{\partial^2 M}{\partial S^2}\right)_Q} = \frac{T}{\left(\frac{\partial T}{\partial S}\right)_Q}. \quad (29)$$

Considering Eqs. (22) and (25), it is a matter of calculation to show that

$$C_Q = \frac{(2\Lambda r_+^2 - m_g^2 c \epsilon r_+ + 2^s (2s-1) \Psi_3) \pi r_+}{4\Lambda r_+^2 - 2^{s+1} \Psi_3}, \quad (30)$$

where

$$\Psi_3 = \begin{cases} \frac{q^2}{l^2} & s = 1 \\ \frac{q}{r_+} & s = \frac{3}{4} \\ \left(\frac{q}{r_+}\right)^{\frac{2(1-s)}{2s-1}} & \text{otherwise} \end{cases} . \quad (31)$$

It is notable that the obtained temperature (22) and the heat capacity (30) consist three terms: cosmological constant, electric charge and massive terms.

According to the obtained heat capacity for cases $s = 1$ and $s = \frac{3}{4}$, we are in a position to find exact bound and phase transition points of AdS black holes. Solving numerator and denominator of the heat capacity with respect to horizon radius leads to following solutions for bound points (r_b) and phase transition points (r_p), respectively,

$$r_b = \begin{cases} \frac{m_g^2 c \varepsilon - \sqrt{m_g^4 c^2 \varepsilon^2 - \frac{16\Lambda q^2}{l^2}}}{4\Lambda} & s = 1 \\ \frac{\Psi_4 + \frac{m_g^4 c^2 \varepsilon^2}{4\Lambda} + m_g^2 c \varepsilon}{4\Lambda} & s = \frac{3}{4} \end{cases} , \quad (32)$$

$$r_p = \begin{cases} \pm \frac{q}{\sqrt{\Lambda}} & s = 1 \\ \frac{(2^{11/4} q \Lambda^2)^{1/3}}{2\Lambda} & s = \frac{3}{4} \end{cases} , \quad (33)$$

where $\Psi_4 = \left(-3^3 2^{3/4} q \Lambda^2 + m_g^6 c^3 \varepsilon^3 + 3^{3/2} \Lambda \sqrt{2^{3/4} q [3^3 2^{3/4} q \Lambda^2 - 2 m_g^6 c^3 \varepsilon^3]}\right)^{1/3}$. Interestingly, phase transition cannot exist for AdS black holes and also it is independent of massive term. Another interesting result is related to the effects of massive term and the electric charge on the bound points of AdS black holes for cases $s = 1$ and $s = \frac{3}{4}$. Considering Eq. (32), it is clear that the bound points increase (decrease) by increasing the charge electric (massive term). Indeed, the physical area decreases for higher charged AdS black holes. It is notable that there is the same behavior for other values of s (see the middle and right panels in Fig. 2). In addition the physical area increases by increasing the value of s (see the left panel in Fig. 2).

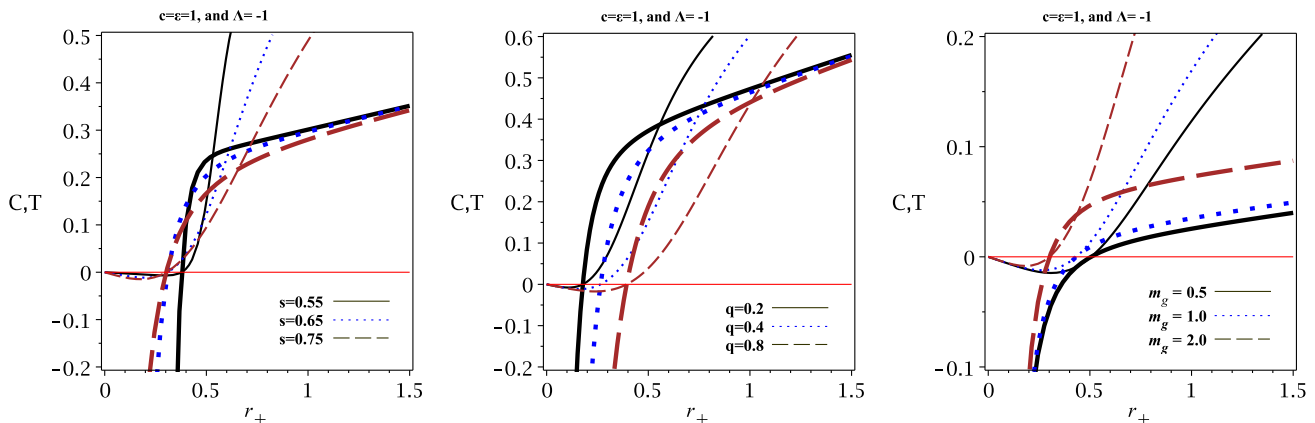


FIG. 2: T (Bold lines) and C_Q (thin lines) versus r_+ for different s (left panel), different q (middle panel) and different m_g (right panel).

V. OPTICAL FEATURES

In this section, we present a careful study of the optical features of AdS black holes in three-dimensional PM-massive theory, such as the shadow geometrical shape, the energy emission rate and the deflection angle. Considering these optical quantities, we investigate the influence of parameters of the theory on the black hole solutions.

A. Photon sphere and shadow

Here, we would like to obtain the radius of photon sphere and spherical shadow for the corresponding black hole and show how they are affected by solution parameters. To this purpose, we employ the Hamilton-Jacobi method for a photon in the black hole spacetime as [134, 135]

$$\frac{\partial \mathcal{S}}{\partial \sigma} + H = 0, \quad (34)$$

where \mathcal{S} and σ are the Jacobi action and affine parameter along the geodesics, respectively. The geodesic motion of a massless photon, in the static spherically symmetric spacetime, can be controlled by the following Hamiltonian

$$H = \frac{1}{2} g^{ij} p_i p_j = 0. \quad (35)$$

Taking into account Eq. (5), the above equation can be written as

$$\frac{1}{2} \left[-\frac{p_t^2}{g(r)} + g(r) p_r^2 + \frac{p_\varphi^2}{r^2} \right] = 0, \quad (36)$$

from which we deduce

$$\dot{p}_t = -\frac{\partial H}{\partial t} = 0, \quad \& \quad \dot{p}_\varphi = -\frac{\partial H}{\partial \varphi} = 0, \quad (37)$$

This shows that Hamiltonian is independent of the coordinates t and φ . So, one can consider p_t and p_φ as constants of motion. We define $-p_t \equiv E$ and $p_\varphi \equiv L$ where E and L are, respectively, the energy and angular momentum of the photon.

Using the Hamiltonian formalism, the equations of motion are given by

$$\dot{t} = \frac{\partial H}{\partial p_t} = -\frac{p_t}{g(r)}, \quad \& \quad \dot{r} = \frac{\partial H}{\partial p_r} = p_r g(r), \quad \& \quad \dot{\varphi} = \frac{\partial H}{\partial p_\varphi} = \frac{p_\varphi}{r^2}, \quad (38)$$

where p_r is the radial momentum and the overdot denotes a derivative with respect to the affine parameter σ . These equations and two conserved quantities provide a complete description of the dynamics by taking into account the orbital equation of motion as follows

$$\dot{r}^2 + V_{\text{eff}}(r) = 0, \quad (39)$$

where V_{eff} is the effective potential of the photon, given by

$$V_{\text{eff}}(r) = g(r) \left[\frac{L^2}{r^2} - \frac{E^2}{g(r)} \right]. \quad (40)$$

It should be noted that the photon orbits are circular and unstable associated to the maximum value of the effective potential. Such a maximum can be obtained by the following conditions

$$V_{\text{eff}}(r_{ph}) = 0, \quad \& \quad V'_{\text{eff}}(r_{ph}) = 0, \quad \& \quad V''_{\text{eff}}(r_{ph}) < 0, \quad (41)$$

where the first two conditions determine the critical angular momentum of the photon sphere (L_p), and the photon sphere radius (r_{ph}), respectively, while the third condition ensures that the photon orbits are unstable.

Taking into account the metric functions (5) and the effective potential (40), $V'_{\text{eff}}(r_{ph}) = 0$ leads to the following relations

$$m_g^2 c \varepsilon r_{ph} - \frac{4q^2}{l^2} \ln \left(\frac{r_{ph}}{l} \right) + \frac{2q^2}{l^2} - 2m_0 = 0 \quad s = 1, \quad (42)$$

$$m_g^2 c \varepsilon r_{ph}^2 + \frac{3q}{2^{\frac{1}{4}}} - 2m_0 r_{ph} = 0 \quad s = \frac{3}{4}, \quad (43)$$

$$(m_g^2 c \varepsilon r_{ph} - 2m_0) (s - 1) + s 2^s (1 - 2s) \left(\frac{q}{r_{ph}} \right)^{\frac{2(1-s)}{2s-1}} = 0 \quad \text{otherwise.} \quad (44)$$

Now, we examine each of above relations separately.

1. $s = 1$: three-dimensional black holes in Maxwell-massive gravity

For the first case, we consider black holes in the Maxwell-massive theory with $s = 1$. Solving Eq. (42) results into the following solution

$$r_{ph} = l \exp \left(\frac{1}{2} - \frac{m_0 l^2}{2q^2} - LambertW \left[-\frac{m_g^2 c \varepsilon l^3}{4q^2} \exp \left(\frac{q^2 - m_0 l^2}{2q^2} \right) \right] \right). \quad (45)$$

In Fig. (3), we depict the relation of the photon sphere radius r_{ph} with respect to the horizon radius r_e for different values of black hole parameters. We can see that r_{ph} grows up to a maximum value with increase of r_e and then gradually reduces as the horizon radius increases more. The place of this maximum can be obtained as

$$r_{e,max} = \frac{c \varepsilon l m_g^2 - \sqrt{c^2 \varepsilon^2 l^2 m_g^4 - 16 \Lambda q^2}}{4 \Lambda l}. \quad (46)$$

According to this fact that the photon sphere radius has to be more than the horizon radius, i.e. $\frac{r_{ph}}{r_e} > 1$ [136], we find that for $r_e < r_{e,max}$, the radius of the photon sphere is an increasing function of r_e which shows that an acceptable optical behavior can be observed in this range. For $r_e > r_{e,max}$, the photon sphere radius is smaller than the horizon radius which is not physically acceptable.

As a next step in the analysis, we investigate the behavior of shadow radius for the corresponding black hole. From the definition of shadow radii [137], the size of black hole shadow can be expressed in celestial coordinates (x, y) as

$$r_{sh} = \sqrt{x^2 + y^2} = \frac{L_p}{E} = \frac{r_{ph}}{\sqrt{g(r_{ph})}}. \quad (47)$$

where L_p is the critical angular momentum of the photon sphere.

According to Eq. (47), a real positive value of the shadow radius is obtained for $g(r_{ph}) > 0$. By rewriting $g(r_{ph})$ in terms of r_e , one finds

$$g = \frac{q^2(2y-1)}{l^2} + c \varepsilon l m_g^2 e^x - \Lambda l^2 e^{2x}, \quad (48)$$

where

$$x = \frac{q^2 + 2q^2 \ln(\frac{r_e}{l}) + \Lambda l^2 r_e^2 - c \varepsilon l^2 m_g^2 r_e - 2q^2 y}{2q^2}, \quad (49)$$

$$y = LambertW \left(-\frac{c \varepsilon l^3 m_g^2 \exp \left(\frac{q^2 + 2q^2 \ln(\frac{r_e}{l}) + \Lambda l^2 r_e^2 - c \varepsilon l^2 m_g^2 r_e}{2q^2} \right)}{4q^2} \right) \quad (50)$$

Our analysis shows that $g(r_{ph})$ is negative for all values of black hole parameters. So according to the Eq. (47), the shadow radii is imaginary, indicating that an acceptable optical behavior cannot be observed for three-dimensional black holes in Maxwell-massive theory of gravity.

2. $s = \frac{3}{4}$: three-dimensional black holes in conformal Maxwell-massive gravity

For the second case, we examine Eq. (43) to study the radius of photon sphere for three-dimensional charged AdS black hole in massive gravity for the nonlinearity parameter $s = \frac{3}{4}$. Solving the equation (43), one can obtain the photon sphere radius in the following form

$$r_{ph} = \frac{2m_0 + \sqrt{4m_0^2 - 2^{\frac{7}{4}} 3m_g^2 c \varepsilon q}}{2m_g^2 c \varepsilon}. \quad (51)$$

To investigate the ratio $\frac{r_{ph}}{r_e}$, we need to determine the horizon radius which is root of the metric function. Our analysis show that the metric function can admit up to three roots as

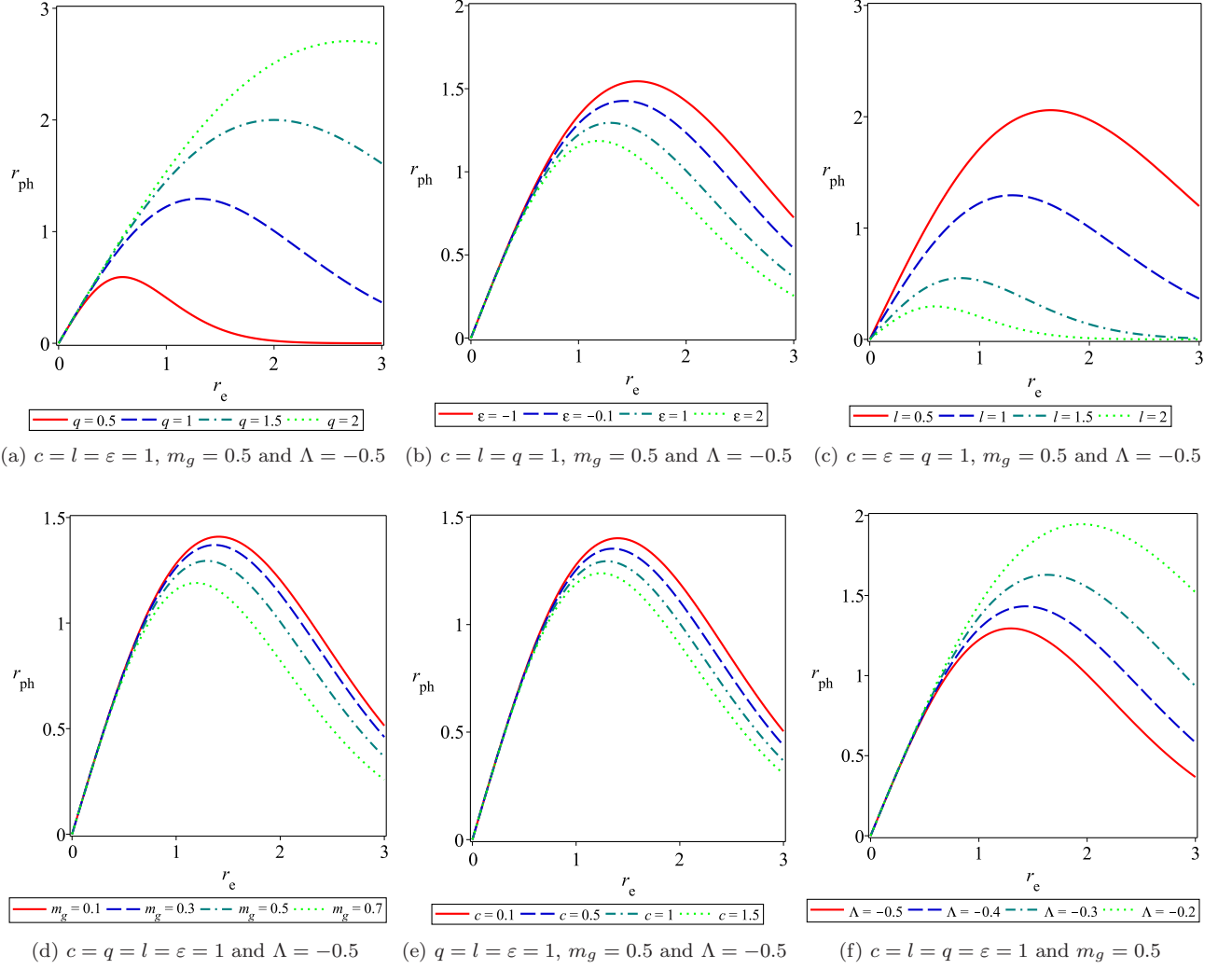


FIG. 3: The radius of photon sphere r_{ph} with respect to the event horizon radius r_e for $s = 1$, $m_0 = 1$ and different values of black hole parameters.

$$r^{(1)} = \frac{2\sqrt{-\Psi_5}}{\sqrt{3}} \sin \left[\frac{1}{3} \sin^{-1} \left(\frac{3\sqrt{3}\Psi_6}{2(\sqrt{-\Psi_5})^3} \right) \right] + \frac{m_g^2 c \varepsilon}{3\Lambda}, \quad (52)$$

$$r^{(2)} = -\frac{2\sqrt{-\Psi_5}}{\sqrt{3}} \sin \left[\frac{1}{3} \sin^{-1} \left(\frac{3\sqrt{3}\Psi_6}{2(\sqrt{-\Psi_5})^3} \right) + \frac{\pi}{3} \right] + \frac{m_g^2 c \varepsilon}{3\Lambda}, \quad (53)$$

$$r^{(3)} = \frac{2\sqrt{-\Psi_5}}{\sqrt{3}} \cos \left[\frac{1}{3} \sin^{-1} \left(\frac{3\sqrt{3}\Psi_6}{2(\sqrt{-\Psi_5})^3} \right) + \frac{\pi}{6} \right] + \frac{m_g^2 c \varepsilon}{3\Lambda}, \quad (54)$$

in which

$$\Psi_5 = -\frac{m_g^4 c^2 \varepsilon^2}{3\Lambda^2} + \frac{m_0}{\Lambda}, \quad (55)$$

$$\Psi_6 = -\frac{2m_g^6 c^3 \varepsilon^3}{27\Lambda^3} + \frac{m_g^2 c \varepsilon m_0}{3\Lambda^2} - \frac{q}{2^{\frac{1}{4}} \Lambda}. \quad (56)$$

According to our analysis, $r^{(2)}$ is always negative and $r^{(3)}$ given by Eq. (54) is the largest positive root.

The ratio of photon sphere radius and horizon radii $\left(\frac{r_{ph}}{r_e}\right)$ is illustrated in Fig. (4). From this figure, one can find that there is a certain region of parameters in which the radius of photon sphere is larger than horizon radius. A remarkable point is that the allowed region of each parameter is dependent on values of other parameters, such that the allowed region reduces with increase of those parameters.

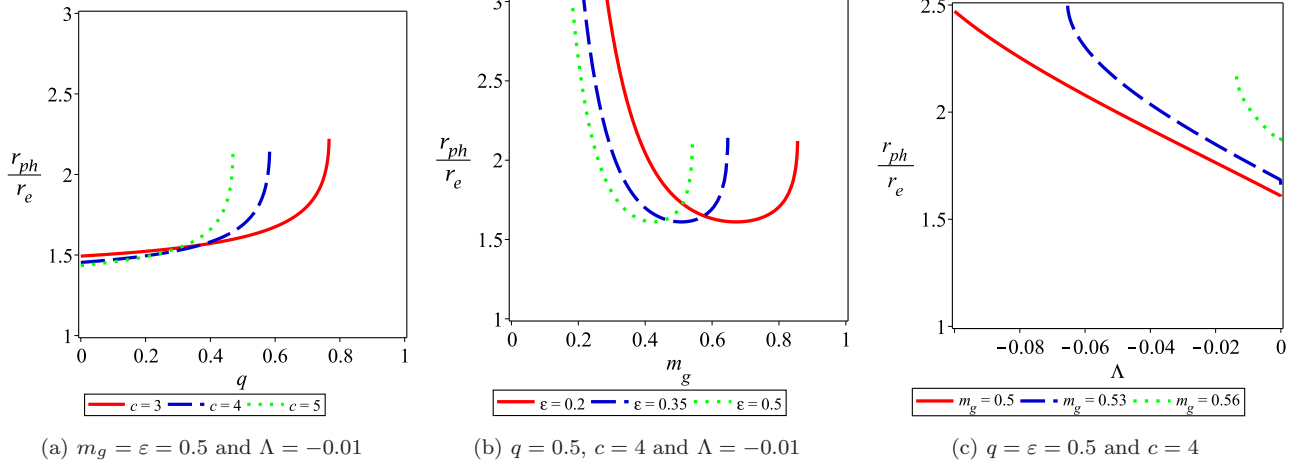


FIG. 4: The dependence of $\frac{r_{ph}}{r_e}$ on the black hole parameters for the nonlinearity parameter $s = \frac{3}{4}$ and $m_0 = 1$.

Inserting Eq. (51) into Eq. (47), we can calculate the radius of black hole shadow. To have an acceptable optical behavior, we need to examine the ratio of shadow radius and photon sphere $\left(\frac{r_{sh}}{r_{ph}}\right)$. Figure 5, gives a simple illustration of how the dependence of this ratio on black hole parameters. As we see from Fig. 5(a), no acceptable optical result is observed for small values of the electric charge and parameter c . Regarding the parameter ε , Fig. 5(b) displays that an admissible optical result can be obtained only for positive values of ε . Taking a look at Fig. 5(c), one can find that such a optical result exist for the small cosmological constant $|\Lambda|$. As a result, one cannot observe an acceptable optical behavior for a black hole located in a weak electric field or high curvature background.

As it was mentioned that each of the parameters has a significant impact on the optical behavior of the system. Fig. 6, displays the effect of parameters on the size of shadow radius. Taking a look at this figure, one can find that the electric charge, graviton mass and parameters ε and c have an decreasing effect on the shadow size. Regarding the effect of cosmological constant, Fig. 6(e) shows that its effect is similar to other parameters. Evidently, as Λ increases from -0.06 to 0 , the radius of shadow decreases. Fig. 6(b), also shows that the effect of the graviton mass is significant on the black hole shadow in comparison with other parameters.

3. $s = \frac{3}{5}$: three-dimensional black holes in PM-massive gravity

Now, we would like to investigate the optical properties of the corresponding black hole for the power parameter $s = \frac{3}{5}$. Considering $s = \frac{3}{5}$ in Eq. (44), we have

$$10m_g^2 c \varepsilon r_{ph}^5 - 20m_0 r_{ph}^4 + 2^{\frac{3}{5}} 3q^4 = 0, \quad (57)$$

We can find the photon sphere radius by solving the above equation. Since this equation is complicated to solve analytically, we employ numerical methods to obtain the horizon radii and the radius of the photon sphere and shadow. In this regard, several values of the event horizon, photon sphere radius, and shadow radius are listed in Table. I. As one can see, only for very limited regions of the electric charge, graviton mass and parameters c and ε , one can observe acceptable optical results, since some constraints are imposed on these parameters due to the imaginary event horizon. Regarding to the cosmological constant, just in a very low curvature background, the photon sphere radius would be smaller than the shadow radii which is physically acceptable. Also, from this table it can be seen that all parameters have a decreasing effect on the event horizon, photon sphere radius and shadow size except the cosmological constant. As we see, r_e and r_{sh} increase by increasing Λ from -0.01 to -0.0005 . Taking a closer look

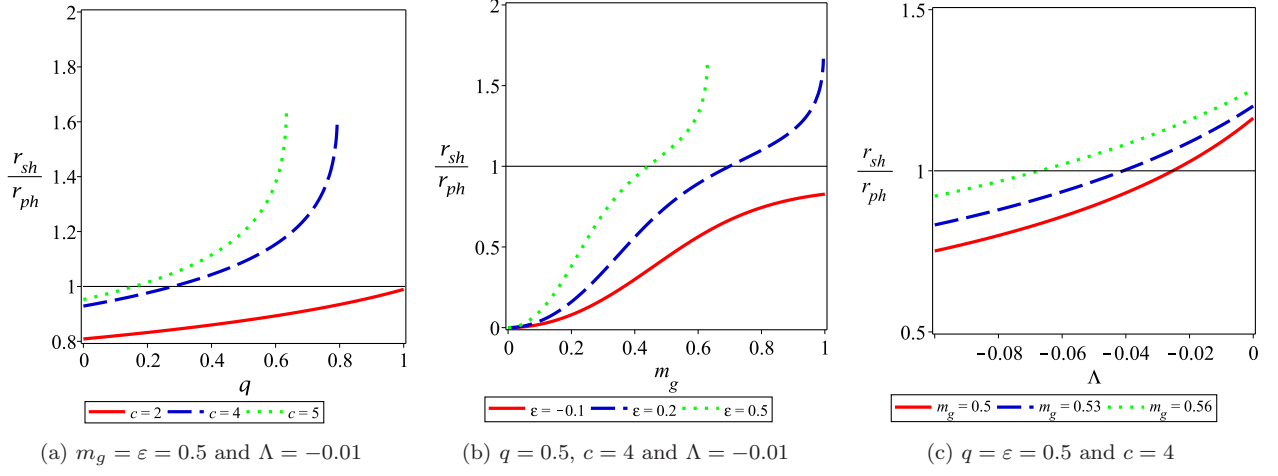


FIG. 5: The dependence of $\frac{r_{sh}}{r_{ph}}$ on the black hole parameters for the nonlinearity parameter $s = \frac{3}{4}$ and $m_0 = 1$.

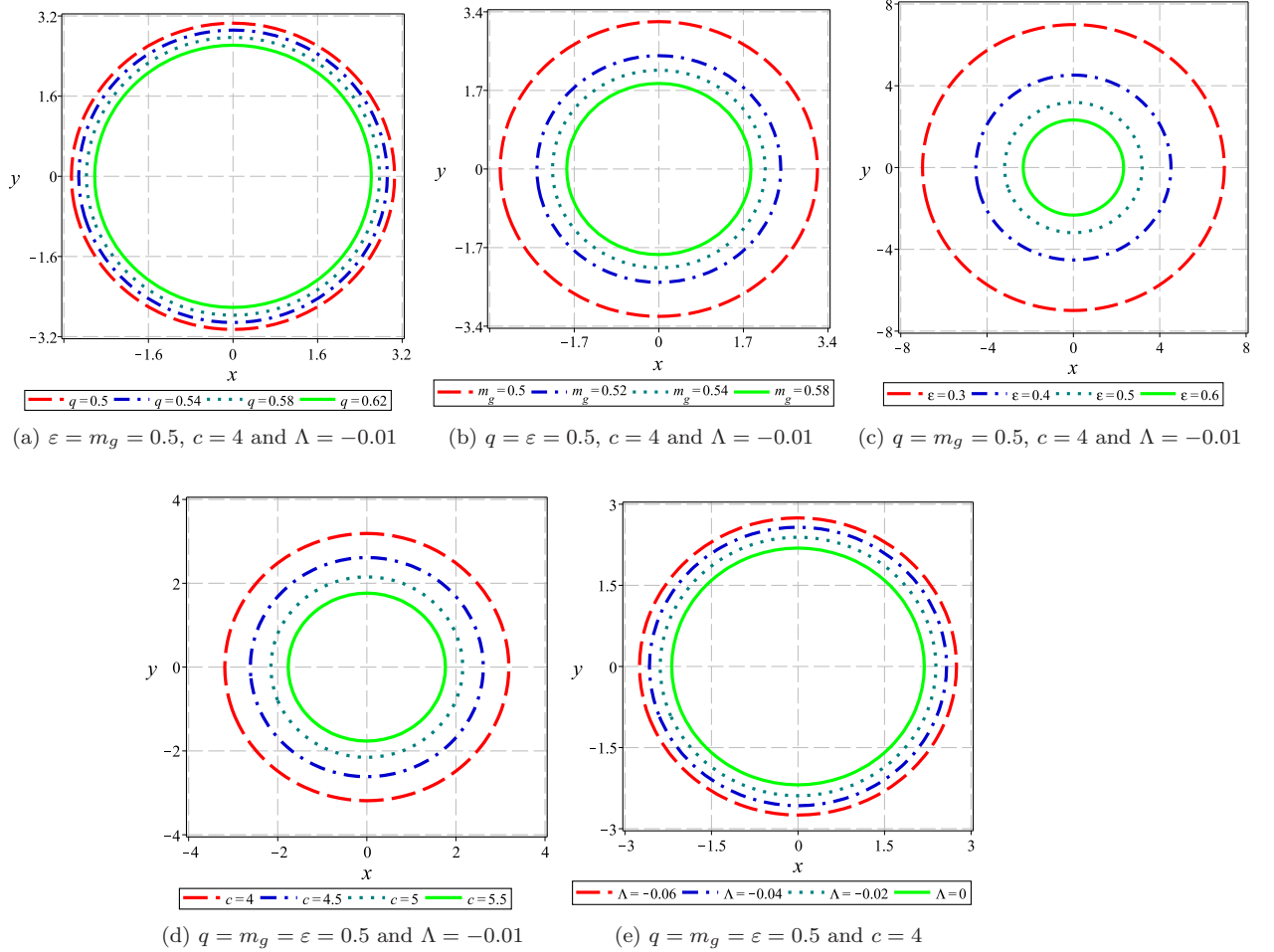


FIG. 6: The black hole shadow in the celestial plane ($x - y$) for the nonlinearity parameter $s = \frac{3}{4}$ and $m_0 = 1$.

at the table, one can notice that the radius of photon sphere is very close to the shadow radius. This reveals the fact that finding an admissible optical behavior is difficult for small values of the nonlinearity parameter.

TABLE I: The event horizon (r_e), photon sphere radius (r_{ph}) and shadow radius (r_{sh}) for the variation of m_g , q , c , ε and Λ for $m_0 = 1$ and $s = \frac{3}{5}$.

m_g	0.7	0.8	0.9	1.1
r_e ($\Lambda = -0.01, q = 0.5, c = 4, \varepsilon = 0.5$)	1.0147	0.7702	0.5935	$0.35 + 0.09I$
r_{ph} ($\Lambda = -0.01, q = 0.5, c = 4, \varepsilon = 0.5$)	2.0391	1.5587	1.2268	0.7973
r_{sh} ($\Lambda = -0.01, q = 0.5, c = 4, \varepsilon = 0.5$)	2.0363	1.5599	1.2323	0.8215
$r_{ph} > r_e$	✓	✓	✓	×
$r_{sh} > r_{ph}$	×	✓	✓	✓
q	0.6	0.7	0.9	1.1
r_e ($\Lambda = -0.01, m_g = 0.7, c = 4, \varepsilon = 0.5$)	1.0097	1.0008	0.9596	$0.83 + 0.12I$
r_{ph} ($\Lambda = -0.01, m_g = 0.7, c = 4, \varepsilon = 0.5$)	2.0373	2.0343	2.0226	1.9982
r_{sh} ($\Lambda = -0.01, m_g = 0.7, c = 4, \varepsilon = 0.5$)	2.0360	2.0355	2.0336	2.0297
$r_{ph} > r_e$	✓	✓	✓	×
$r_{sh} > r_{ph}$	×	✓	✓	✓
c	4	5	6	8
r_e ($\Lambda = -0.01, m_g = 0.7, q = 0.5, \varepsilon = 0.5$)	1.0147	0.8066	0.6633	$0.37 + 0.06I$
r_{ph} ($\Lambda = -0.01, m_g = 0.7, q = 0.5, \varepsilon = 0.5$)	2.0391	1.6293	1.3548	0.8861
r_{sh} ($\Lambda = -0.01, m_g = 0.7, q = 0.5, \varepsilon = 0.5$)	2.0363	1.6299	1.3583	0.9032
$r_{ph} > r_e$	✓	✓	✓	×
$r_{sh} > r_{ph}$	×	✓	✓	✓
ε	0.6	0.7	0.9	1.1
r_e ($\Lambda = -0.01, m_g = 0.7, q = 0.5, c = 4$)	0.8417	0.7153	0.5336	$0.37 + 0.05I$
r_{ph} ($\Lambda = -0.01, m_g = 0.7, q = 0.5, c = 4$)	1.6971	1.4530	1.1236	0.9082
r_{sh} ($\Lambda = -0.01, m_g = 0.7, q = 0.5, c = 4$)	1.6944	1.4554	1.1313	0.9241
$r_{ph} > r_e$	✓	✓	✓	×
$r_{sh} > r_{ph}$	×	✓	✓	✓
Λ	-0.01	-0.005	-0.001	-0.0005
r_e ($\varepsilon = 0.5, m_g = 0.7, q = 0.5, c = 4$)	1.0147	1.0153	1.0157	1.0158
r_{ph} ($\varepsilon = 0.5, m_g = 0.7, q = 0.5, c = 4$)	2.0391	2.0391	2.0391	2.0391
r_{sh} ($\varepsilon = 0.5, m_g = 0.7, q = 0.5, c = 4$)	2.0363	2.0384	2.0401	2.0403
$r_{ph} > r_e$	✓	✓	✓	✓
$r_{sh} > r_{ph}$	×	×	✓	✓

B. Energy emission rate

In this subsection, we are interested in studying the associated energy emission rate. It has been known that the black hole shadow corresponds to its high energy absorption cross-section for a far distant observer [138, 139]. In fact, at very high energies, the absorption cross-section oscillates around a limiting constant value σ_{lim} which is defined in the following form for an arbitrary dimensional spacetime

$$\sigma_{lim} = \frac{\pi^{\frac{d-2}{2}} r_{sh}^{d-2}}{\Gamma(\frac{d}{2})}. \quad (58)$$

The energy emission rate for three-dimensional spacetime is expressed as

$$\frac{d^2 E(\omega)}{dt d\omega} = \frac{4\pi^2 \omega^2 r_{sh}}{e^{\frac{\omega}{T}} - 1}, \quad (59)$$

in which ω is the emission frequency and T denotes the Hawking temperature. For the case $s = \frac{3}{4}$, Hawking temperature is calculated as

$$T = \frac{1}{4\pi} \left(m_g^2 c \varepsilon - 2\Lambda r_e - \frac{q}{2^{\frac{1}{4}} r_e^2} \right). \quad (60)$$

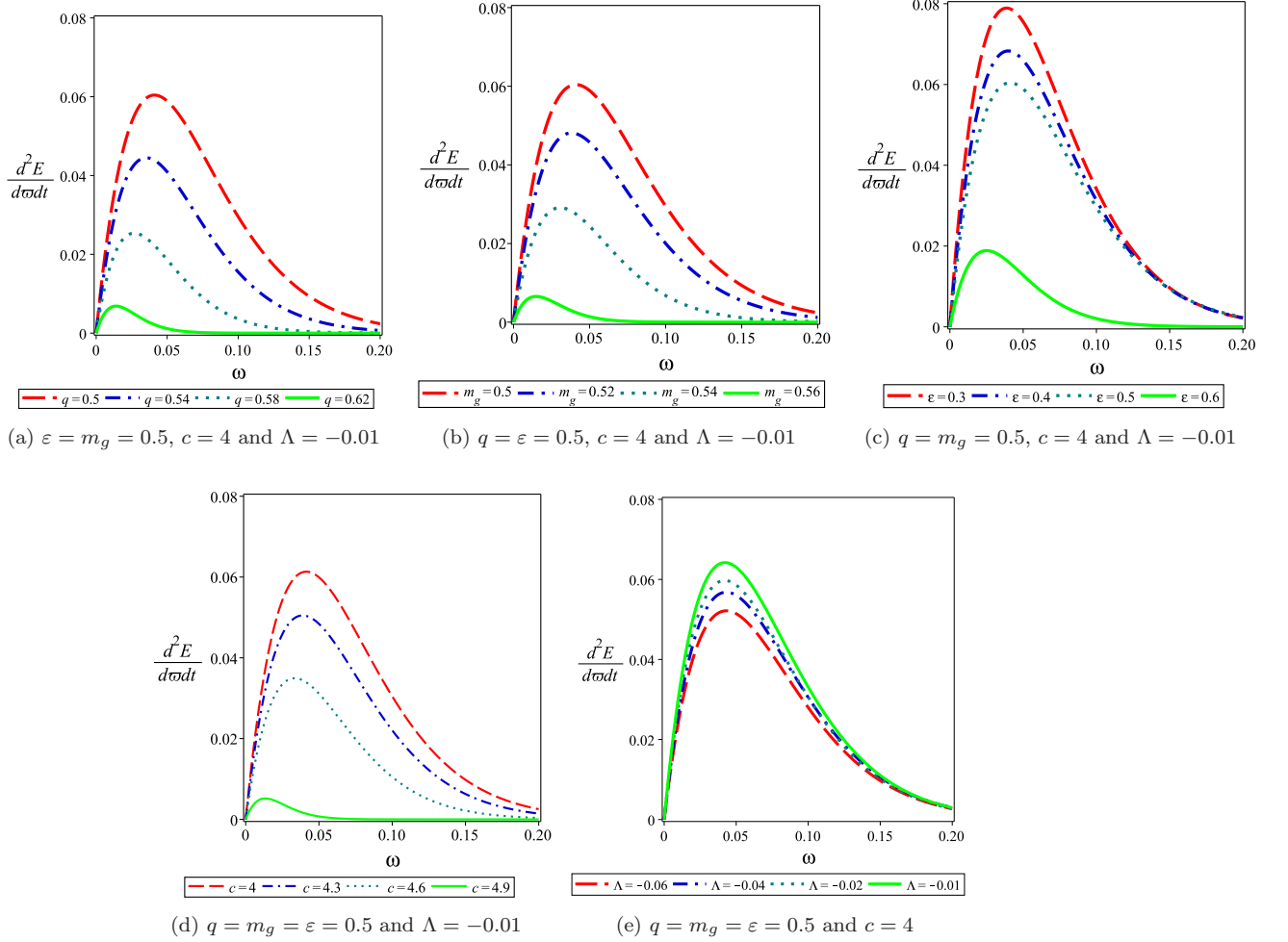


FIG. 7: Energy emission rate for the corresponding black hole with $s = \frac{3}{4}$, $m_0 = 1$ and different values of black hole parameters.

The qualitative behavior of the energy emission rate is illustrated in Fig. 7, as a function of ω for different values of parameters. Taking a look at this figure, one can see that there exists a peak of the energy emission rate which decreases and shifts to the low frequency with the increase (decrease) of the electric charge, graviton mass, the parameters c and ε (the cosmological constant). As one can see from Fig. 7(a), the electric charge decreases the energy emission, meaning that the evaporation process would be slower for a black hole located in a more powerful electric field. The effect of graviton mass on the emission rate is depicted in Fig. 7(b) which shows that emission of particles becomes insignificant for massive gravitons. Regarding the effects of the parameters c and ε , Figs. 7(c) and 7(d) display that increasing these two parameters results in the decrease of the energy emission. In other words, decreasing these parameters implies a fast emission of particles. To examine the influence of the cosmological constant, we depict Fig. 7(e) which illustrates that this parameter has an increasing contribution on the emission rate unlike other parameters. In fact, by increasing Λ from -0.06 to -0.01 , the energy emission rate grows. This reveals the fact that when the black hole is located in a low curvature background, the evaporation process would be faster. From what was expressed, one can find that the black hole has a longer lifetime for massive gravitons or when it is located in a high curvature background or in a powerful electric field.

C. Deflection angle

Here, we proceed to study the deflection angle of light by using the null geodesics method [140–143]. The total deflection Θ can be determined by the following relation

$$\Theta = 2 \int_b^\infty \left| \frac{d\varphi}{dr} \right| dr - \pi, \quad (61)$$

in which b is the impact parameter, defined as $b \equiv L/E$. Using equations of motion (38), we have

$$\left| \frac{d\varphi}{dr} \right| = \frac{\dot{\varphi}}{\dot{r}} = \frac{b}{r^2} \left(1 - \frac{b^2 g(r)}{r^2} \right)^{-\frac{1}{2}}. \quad (62)$$

Inserting Eq. (62) into Eq. (61), one can calculate the deflection angle as

$$\begin{aligned} \Theta = & \frac{3\sqrt{2}q^2}{56b^2} + \frac{2^{\frac{3}{4}}q(1-m_0)}{8b} + \frac{6-m_0}{3} + \frac{3\left(m_0^2 + 2^{\frac{3}{4}}m_g^2c\varepsilon q\right)}{20} - \frac{3bq\Lambda}{2^{\frac{13}{4}}} \\ & + \frac{bm_g^2c\varepsilon(4-m_0)}{8} - \frac{\Lambda b^2(2-m_0)}{2} - \frac{3\Lambda b^3(m_g^2c\varepsilon - b\Lambda)}{4}. \end{aligned} \quad (63)$$

To show the effects of different parameters on the deflection angle, we have depicted Fig. 8, which displays the variation of the deflection angle Θ as a function of the parameter b for different values of black hole parameters. As one can see, all curves reduce to a minimum value with increase of b and then gradually grow as the impact parameter increases more. In other words, they have a global minimum value, meaning that there exists a finite value of the impact parameter b which deflection of light is very low for it. According to the relation $b \equiv L/E$, this finite value is dependent on the values of angular momentum and energy of the photon. Fig. 8(a) illustrates the increasing effect of the electric charge on the deflection angle. This shows that deflection of light will be very high in the presence of a powerful electric field. To examine the impact of graviton mass, we have plotted Fig. 8(b) which indicates that photons get deflected more than their straight path in the presence of massive gravitons. Regarding to the effects of parameters c and ε , the increasing of these two parameters leads to the increasing of the deflection angle (see Figs. 8(c) and 8(d), for more details). Studying Λ effect, we observe that as Λ increases from -0.06 to -0.01 , the deflection angle decreases. This shows that deflection of light is low in a background with low curvature. Comparing all of panels in Fig. 8, we notice that the effect of electric charge is notable for small values of the impact parameter, whereas other parameters have a significant effect for large values of b .

VI. CONNECTION BETWEEN SHADOW RADIUS AND QUASINORMAL MODES

One of the interesting dynamic properties of black holes is quasinormal modes (QNMs) which are the response of black holes to external perturbations. In fact, black holes interact with matter and radiations in surroundings and as a result of these interactions, they take a perturbed state. A perturbed black hole tends to relax towards equilibrium through the emission of QNMs. QNMs are complex frequencies, $\omega = \omega_R - i\omega_I$, which encode important information related to the stability of the black hole under small perturbations. The sign of the imaginary part determines if the mode is stable or unstable. If $\omega_I > 0$ (exponential growth), the mode is unstable, whereas for $\omega_I < 0$ (exponential decay) it is stable. For a stable mode, the real part provides the frequency of oscillation, while the inverse of $|\omega_I|$ determines the dumping time $t_D^{-1} = |\omega_I|$ [144]. Recently, it has been suggested that the real part of QNMs in the eikonal limit corresponds to the radius of the black hole shadow [145, 146]. In fact, the real and imaginary parts of QNMs in such a limit are, respectively, related to the angular velocity and Lyapunov exponent of unstable circular null geodesics. It should be noted that such a correspondence is only guaranteed for test fields, and not for gravitational ones [147]. This topic has received much interest in studying different black holes [148–150].

In this section, we employ this idea and investigate small scalar perturbations around the black hole solution. According to this correspondence, the quasinormal frequency ω can be calculated with the property of the photon sphere as [151]

$$\omega = \ell\Omega - i \left(n + \frac{1}{2} \right) |\lambda|, \quad (64)$$

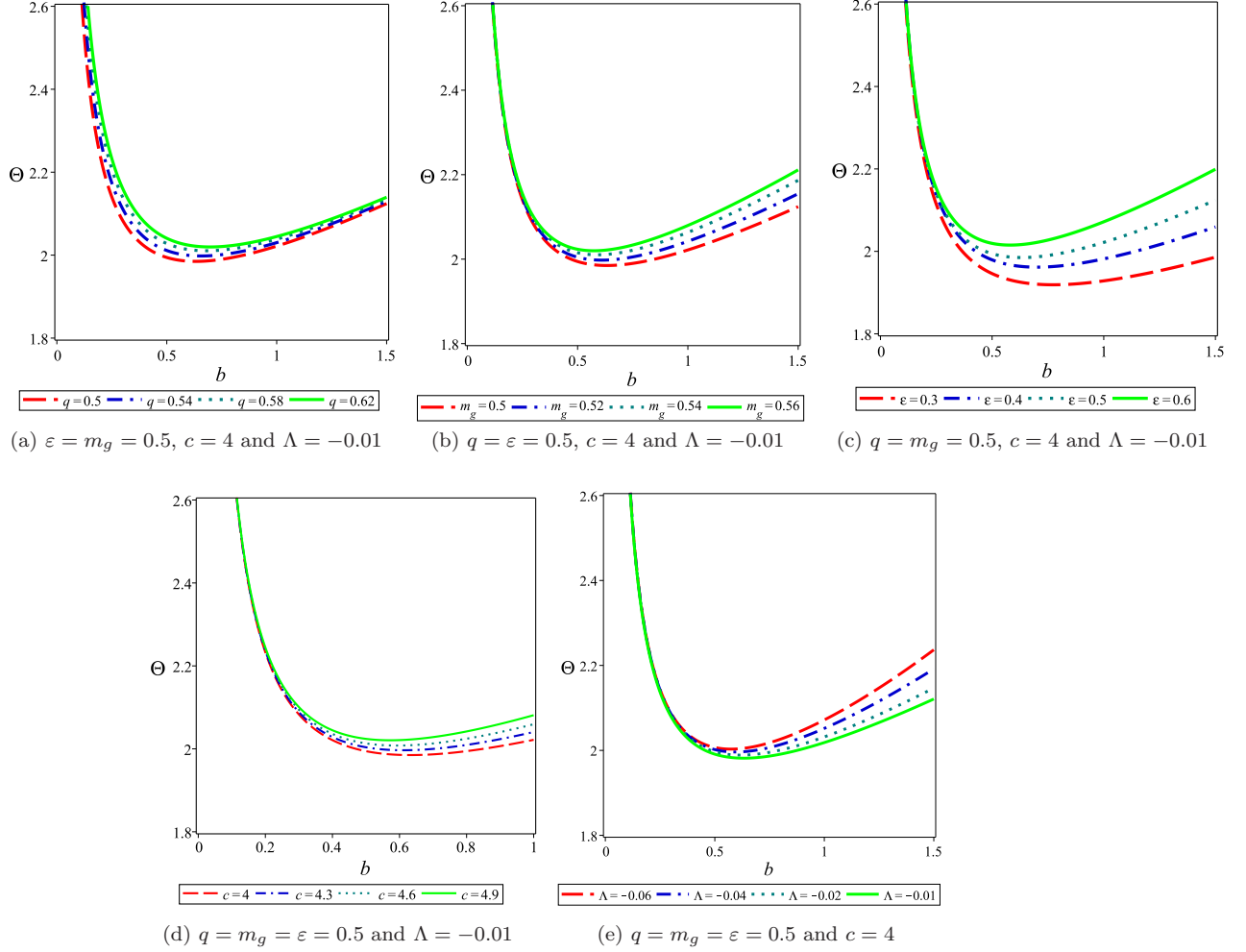


FIG. 8: The behavior of Θ with respect to the impact parameter b for $s = \frac{3}{4}$, $m_0 = 1$ and different values of BH parameters.

in which n and ℓ are, respectively, the overtone number and angular quantum number. Ω is the coordinate angular velocity given as

$$\Omega = \frac{\dot{\varphi}}{\dot{t}} = \sqrt{\frac{g(r_{ph})}{r_{ph}^2}} = \frac{1}{r_{sh}}, \quad (65)$$

and Lyapunov exponent λ is interpreted as the decay rate of the unstable circular null geodesics and expressed as

$$\lambda = \frac{\sqrt{2g(r_{ph}) - r_{ph}^2 g''(r_{ph})}}{\sqrt{2}r_{sh}}. \quad (66)$$

Taking Eqs. (47) and (51) into account, we are in a position to investigate how the black hole parameters affect QNM frequencies. These effects are illustrated in Fig. (9), where the spectrum obtained exhibits the following features:

- The real (imaginary) part of QNM frequencies is an increasing (a decreasing) function of the graviton mass. This shows that the scalar field perturbations around the black hole oscillate with more energy for massive gravitons and since $|\omega_I| = t_D^{-1}$ they decay faster.

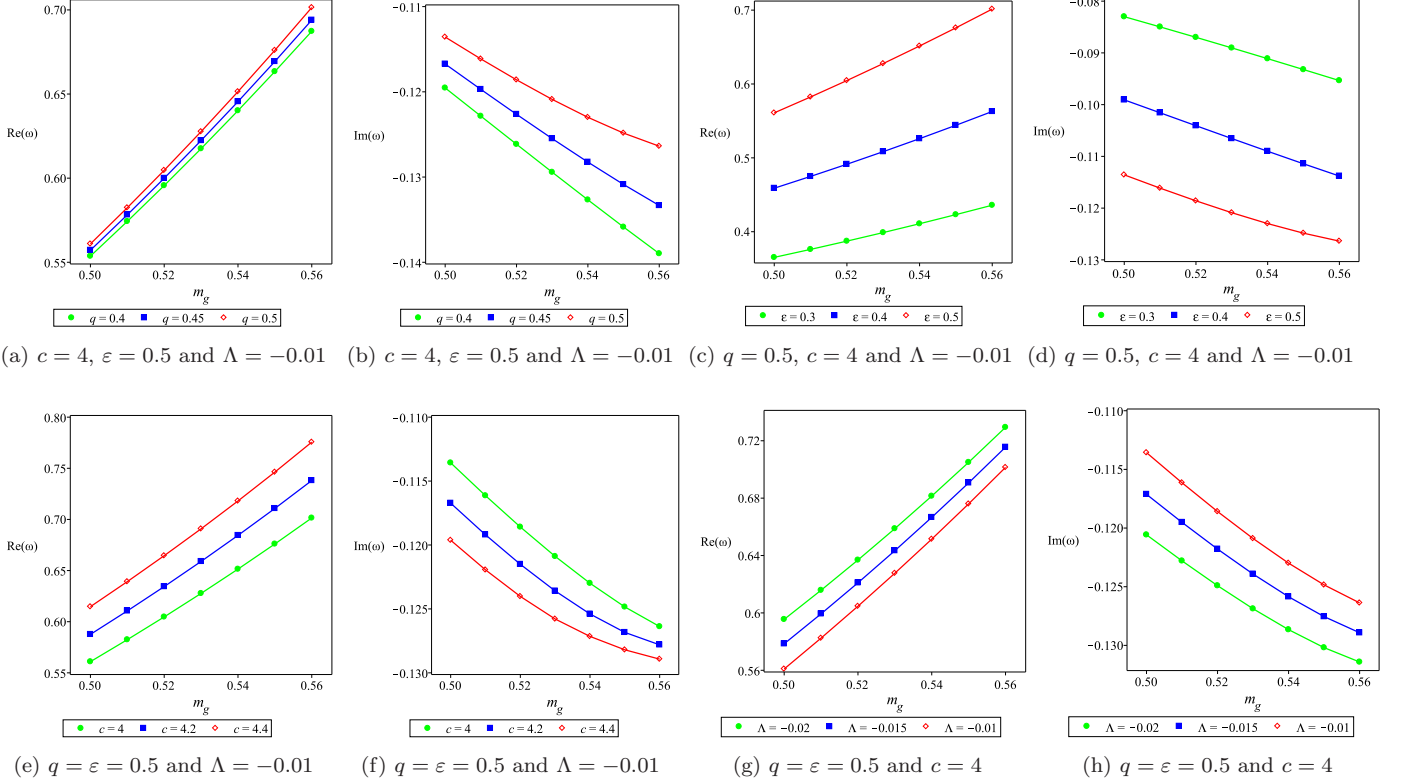


FIG. 9: The behavior of $Re(\omega)$ and $Im(\omega)$ with respect to the graviton mass for $m_0 = 1$, $n = 0$, $\ell = 2$, $s = 3/4$ and different values of q (Figs. 9a and 9b), ε (Figs. 9c and 9d), c (Figs. 9e and 9f) and Λ (Figs. 9g and 9h).

- According to panels (a) and (b) in Fig. 9, increasing of the electric charge leads to increasing both real and imaginary parts of the QNM frequency. This reveals the fact that the scalar field perturbations in the presence of the large electric charge oscillate faster and decay slower.
- Panels (c) and (d) in Fig. 9, indicate that by increasing the parameter ε , the real (imaginary) value of QNM frequency increases (decreases). This indicates that as the effect of this parameter gets stronger, the energy of QNMs grows but, with a shorter lifetime, they decay faster.
- $Re(\omega)$ ($Im(\omega)$) increases (decreases) by increasing the parameter c , which is transparent from panels (e) and (f) in 9.
- According to panels (g) and (h) in Fig. 9, as the cosmological constant increases from -0.02 to -0.01 , the real (imaginary) part of QNM decreases (increases), meaning that the scalar perturbations have less energy for oscillations and decay slower in a lower curvature background.

VII. QUASINORMAL MODES OF MASSIVE PARTICLES

In the present section we will investigate how the quasinormal modes are disturbed for massive particles. In what follow we will summarize the main ingredients as well as the method utilized to make progress. Up to now, quasinormal modes have been considered in different contexts, backgrounds and also different dimensions [152–155]. However, should be mentioned the seminal papers regarding this topic long time ago [156, 157].

Let us start by considering the propagation of a test scalar field, Φ in a well-known three-dimensional gravitational background. The above-mentioned field: i) it is assumed to be real, ii) it is massive, iii) it is electrically neutral, and finally iv) Φ is minimally coupled to gravity. Thus, the action $S[g_{\mu\nu}, \Phi]$ can be written in the simplest form

$$S[g_{\mu\nu}, \Phi] \equiv \frac{1}{2} \int d^3x \sqrt{-g} \left[\partial^\mu \Phi \partial_\mu \Phi + m_s^2 \Phi^2 \right],$$

being m_s the mass of the scalar field. Utilizing the Klein-Gordon equation (see [158–161] and references therein)

$$\frac{1}{\sqrt{-g}}\partial_\mu(\sqrt{-g}g^{\mu\nu}\partial_\nu)\Phi = m_s^2\Phi. \quad (67)$$

Be aware and notice we can fix the background and then, the corresponding backreaction is neglected. Now, to decouple and resolve the Klein-Gordon equation, we take advantage of the method of separation of variables. Thus, we assume the ansatz

$$\Phi(t, r, \phi) = e^{-i\omega t + im\phi} \frac{y(r)}{r^{1/2}}, \quad (68)$$

where ω is the unknown frequency (which will be determined), while m is a quantum number of the angular coordinate ϕ . After the use of the ansatz it is easy to obtain, for the radial part, a Schrödinger-like equation, i.e.,

$$\frac{d^2y}{dx^2} + [\omega^2 - V(x)]y = 0, \quad (69)$$

where x is the well-known tortoise coordinate, i.e.,

$$x \equiv \int \frac{dr}{f(r)}, \quad (70)$$

We have defined an effective potential (for scalar perturbations) in three dimensions, given by [162]

$$V(r) = f(r) \left(m_s^2 + \frac{f'(r)}{2r} - \frac{f(r)}{4r^2} + \frac{m^2}{r^2} \right). \quad (71)$$

As always, the prime denotes differentiation with respect to the radial coordinate. As is obvious, this effective potential depends on the constant parameters of the theory m , m_s , and the black hole parameters m_0 , Λ , c , ε , s and also m_g . Be aware and notice that the power s and the scalar mass m_s are not related, i.e., s and m_s are selected independently. Along this manuscript, we have three different values for the lapse function, depending on the power s . To be consistent, we will restrict our analysis to the case in which $s = 3/4$. Thus, we plot the effective potential for different cases of the parameters involved in Fig. 10.

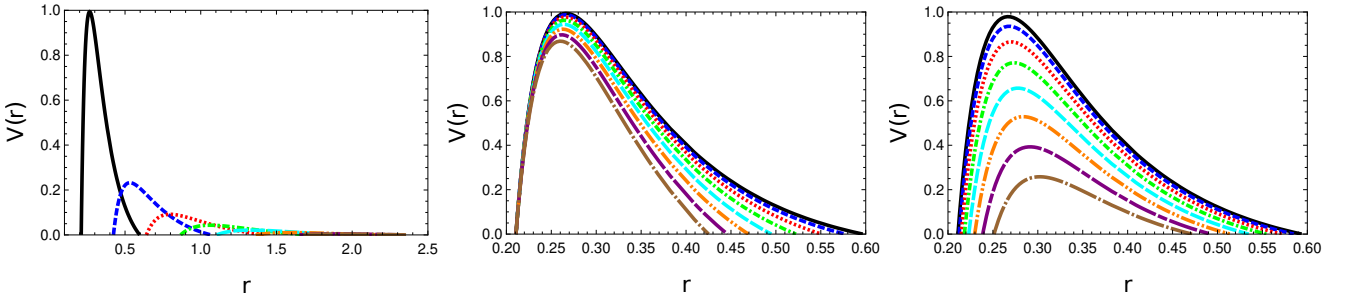


FIG. 10: **Left panel:** Effective potential for $m_0 = 1$, $\Lambda = -1/5^2$, $m_g = 0$, $c = 1$, $\varepsilon = 1$, $m = 0$, $m_s = 0.1$ and: $q = 0.25$ (solid black hole), $q = 0.50$ (dashed blue line), ..., $q = 2.00$ (long dotted-dashed brown line). **Middle panel:** Effective potential for $m_0 = 1$, $\Lambda = -1/5^2$, $m_g = 0$, $c = 1$, $\varepsilon = 1$, $q = 0.25$, $m = 0$ and: $m_s = 0.1$ (solid black line), $m_s = 0.2$ (dashed blue line), ..., $m_s = 0.8$ (long dotted-dashed brown line). **Right panel:** Effective potential for $m_0 = 1$, $\Lambda = -1/5^2$, $c = 1$, $\varepsilon = 1$, $q = 0.25$, $m = 0$, $m_s = 0.1$ and: $m_g = 0.1$ (solid black line), $m_g = 0.2$ (dashed blue line), ..., $m_g = 0.8$ (long dotted-dashed brown line).

Given that the WKB method is very well-known, we take advantage of such a fact to circumvent unnecessary details. From the literature we know that QN spectra may be computed by means of the following expression

$$\omega_n^2 = V_0 + (-2V_0'')^{1/2}\Lambda(n) - i\nu(-2V_0'')^{1/2}[1 + \Omega(n)], \quad (72)$$

where the symbols have the following meaning: i) $\nu = n + 1/2$, ii) V_0 is the maximum of the effective potential, iii) $n = 0, 1, 2, \dots$ is the overtone number, iv) V_0'' is the second derivative of the potential evaluated at the maximum. The

remaining functions $\Lambda(n), \Omega(n)$ are complex expressions of ν and derivatives of the potential (at the maximum), see [163, 164] and references therein. We have used the Wolfram Mathematica [165] code utilizing WKB method [166].

Our numerical results are summarized in Fig. 11, as well as in the Table. II. We then show the corresponding QNMs in different cases by plotting: i) the real part against the imaginary part. ii) the real part vs the parameters q, m_s and m_g . iii) the imaginary part vs the parameters q, m_s and m_g . We have considered the simplest case ($n = 0$) in all cases. We observe that all the modes are found to be stables.

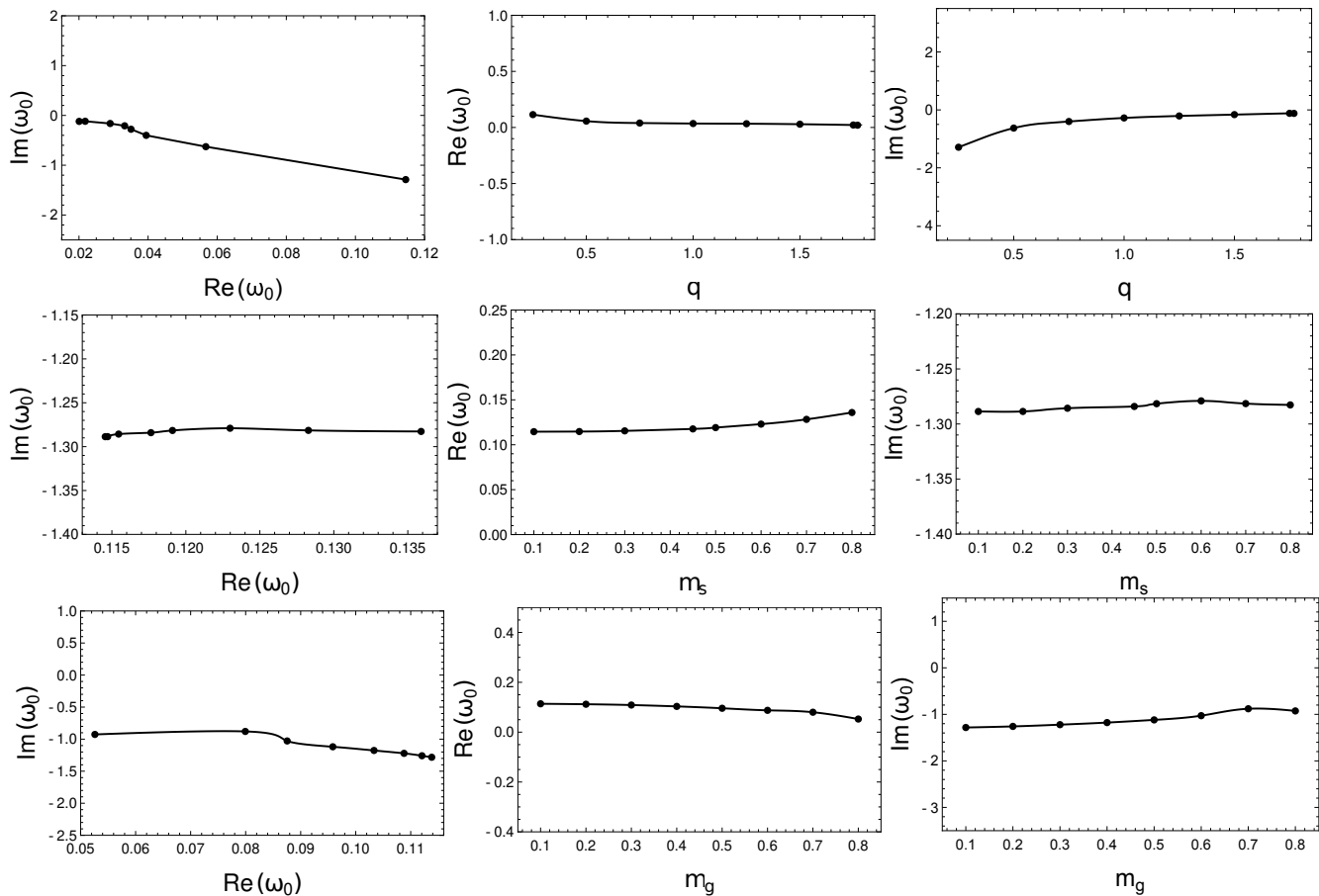


FIG. 11: The figure shows three different sub-plots: Plot of $\text{Im}(\omega_0)$ vs $\text{Re}(\omega_0)$, Plot of $\text{Re}(\omega_0)$ vs $\{q, m_s, m_g\}$, and Plot of $\text{Im}(\omega_0)$ vs $\{q, m_s, m_g\}$. **Up panel:** Figures obtained assuming $m_0 = 1, \Lambda = -1/5^2, m_g = 0, c = 1, \varepsilon = 1, m = 0, m_s = 0.1$ and a variable q . **Middle panel:** Figures obtained assuming $m_0 = 1, \Lambda = -1/5^2, m_g = 0, c = 1, \varepsilon = 1.0, q = 0.25, m = 0$ and a variable m_s . **Down panel:** Figures obtained assuming $m_0 = 1, \Lambda = -1/5^2, c = 1, \varepsilon = 1.0, q = 0.25, m = 0, m_s = 0.1$ and a variable m_g .

VIII. CONCLUSIONS

In this paper, we have considered three-dimensional charged black holes in the PM-massive gravity context. After an short introduction, we have computed the exact black hole solution and investigated several physical properties of this black hole. Studying the thermodynamic behavior of the solution, we examined its thermal stability and phase transition by calculating the heat capacity in a canonical ensemble. Then, we performed an in-depth analysis of the optical features of the corresponding black hole including the shadow radius, energy emission rate and deflection angle, and inspected the influence of the model's parameters on the considered optical quantities. Furthermore, we have computed the QNMs following two alternative perspectives and showed that all modes are found to be stables. Also, it is important to point out that, although we have obtained the complete analytic solution, the case $s = 3/4$ is the most interesting given that in such value the trace of the energy momentum tensor vanished.

In studying the photon sphere and shadow radius of the black hole, we noticed that an acceptable optical behavior cannot be observed for three-dimensional black holes in the Maxwell-massive theory. Regarding to the three-

TABLE II: QN frequencies for scalar perturbations for the three cases considered above.

q	ω_0
0.25	0.11455148097649198 - 1.2886523135636836 I
0.50	0.05670941157920715 - 0.6277162004759173 I
0.75	0.03944782649614513 - 0.4000845881573267 I
1.00	0.03506029693925167 - 0.2774177913064879 I
1.25	0.03321551664735227 - 0.2089577449836478 I
1.50	0.02901810442718903 - 0.1622820052593347 I
1.75	0.02179974078482501 - 0.1175878901489007 I
1.77	0.02005797350192942 - 0.1200543084446637 I
m_s	ω_0
0.10	0.11455148097649198 - 1.2886523135636836 I
0.20	0.11471431131320475 - 1.2886131548231460 I
0.30	0.11545694183477717 - 1.2856934694434503 I
0.45	0.11764064465653681 - 1.2840853329458881 I
0.50	0.11909651321939323 - 1.2815831339247148 I
0.60	0.12298731842270087 - 1.2790403627402582 I
0.70	0.12828210406856083 - 1.2814841985525631 I
0.80	0.13589908351543734 - 1.2827041639445738 I
m_g	ω_0
0.10	0.11382024326493657 - 1.2823703727231917 I
0.20	0.11204575012625576 - 1.2588767018795977 I
0.30	0.10879218321968893 - 1.2214540133449208 I
0.40	0.10333047591342347 - 1.1765523839144725 I
0.50	0.09584148861224073 - 1.1188674717779419 I
0.60	0.08754639019329823 - 1.0281847011650955 I
0.70	0.07993449356477120 - 0.8795062900915184 I
0.80	0.05259931400161963 - 0.9263197561456396 I

dimensional charged black holes in PM-massive gravity, our analysing showed that an admissible optical result can be obtained for special regions of black hole parameters. Worth mentioning that such an admissible optical result is observable only for intermediate values of the nonlinearity parameter s . Studying the impact of the black hole parameters on the radius of black hole shadow, we found that all parameters have decreasing contribution on the shadow size.

Then, we continued by studying the energy emission rate and explored the effect of black hole parameters on the radiation process. The results indicated that as the graviton mass and parameters c and ε increase, the emission of particles around the black hole decreases. This revealed the fact that the radiation rate grows when the effects of these parameters get weaker. Regarding the effects of electric charge and cosmological constant, we noticed that the evaporation process would be slow for a black hole located in a powerful electric field or in a background with higher curvature. In other words, the lifetime of a black hole would be longer under such conditions.

Furthermore, we presented a study in the context of the gravitational lensing of light around these black holes. Depending on the values of black hole parameters and impact parameter, photons get deflected from their straight path and have different behaviors. For small values of the impact parameter b , the deflection angle was a decreasing function of b , whereas for large values, it was an increasing function. This shows that there exists a global minimum value of the impact parameter b which deflection of light is very low for it. Relative to the impact of electric charge, we found that it has an increasing contribution on the deflection angle Θ . In other word, deflection of light in the presence of the large electric charge is very high as compared to black holes located in a weak electric field. We also

noticed that the effects of graviton mass and parameters c and ε on the deflection angle are similar to that of the electric charge. Whereas the cosmological constant exhibited decreasing effects on Θ , meaning that deflection of light is low in a background with low curvature.

In addition, we employed the connection between the shadow radius and quasinormal modes and investigated small perturbations around the black holes. We found that: i) Increasing the electric charge lead to increasing both real and imaginary parts of the QNM frequency. This revealed the fact that the scalar field perturbations in the presence of a powerful electric field oscillate faster and decay more slowly. ii) As the graviton mass and parameters c and ε increase the real (imaginary) part of the quasinormal frequencies increase (decrease). This means that as the effect of massive gravitons and parameters c and ε get stronger, the energy of the QNMs grows and they decay faster. iii) The effect of cosmological constant is to decrease (increase) the real (imaginary) part of the QNMs. This shows that although the scalar field perturbations have less energy for oscillation in a lower curvature background, they decay slower in such a situation.

Acknowledgments

BEP thanks University of Mazandaran. Also AR acknowledges Universidad de Tarapacá for financial support.

-
- [1] B. Eslam Panah, Europhys. Lett. 134 (2021) 20005.
 - [2] M. Banados, C. Teitelboim, and J. Zanelli, Phys. Rev. Lett. 69 (1992) 1849.
 - [3] E. Witten, Adv. Theor. Math. Phys. 2 (1998) 505.
 - [4] H. -W. Lee, Y. -S. Myung, and J. -Y. Kim, Phys. Lett. B 466 (1999) 211.
 - [5] A. Larranaga, Commun. Theor. Phys. 50 (2008) 1341.
 - [6] S. Carlip, Class. Quantum Gravit. 12 (1995) 2853.
 - [7] R. -G. Cai, and J. -H. Cho, Phys. Rev. D 60 (1999) 067502.
 - [8] A. Ashtekar, J. Wisniewski, and O. Dreyer, Adv. Theor. Math. Phys. 6 (2003) 507.
 - [9] T. Sarkar, G. Sengupta, and B. Nath Tiwari, J. High Energ. Phys. 11 (2006) 015.
 - [10] M. Cadoni, and C. Monni, Phys. Rev. D 80 (2009) 024034.
 - [11] M. Akbar, H. Quevedo, K. Saifullah, A. Sanchez, and S. Taj, Phys. Rev. D 83 (2011) 084031.
 - [12] E. Witten, *Three-Dimensional Gravity Revisited*, [arXiv:0706.3359].
 - [13] M. A. Anacleto, F. A. Brito, and E. Passos, Phys. Lett. B 743 (2015) 184.
 - [14] R. Emparan, G.T. Horowitz, and R.C. Myers, J. High Energ. Phys. 01 (2000) 021.
 - [15] S. Carlip, Class. Quantum Gravit. 22 (2005) R85.
 - [16] E. Frodden, M. Geiller, K. Noui, and A. Perez, J. High Energ. Phys. 05 (2013) 139.
 - [17] D. V. Singh, and S. Siwach, Class. Quantum Grav. 30 (2013) 235034.
 - [18] P. Caputa, V. Jejjala, and H. Soltanpanahi, Phys. Rev. D 89 (2014) 046006.
 - [19] T. Jurić, and A. Samsarov, Phys. Rev. D 93 (2016) 104033.
 - [20] B. Eslam Panah, S. Panahiyan, and S. H. Hendi, Prog. Theo. Exp. Phys. 2019 (2019) 013E02.
 - [21] R. Emparan, A. M. Frassino, and B. Way, J. High Energ. Phys. 11 (2020) 137.
 - [22] C. Germani, and G. P. Procopio, Phys. Rev. D 74 (2006) 044012.
 - [23] A. de la Fuente, and R. Sundrum, J. High Energ. Phys. 09 (2014) 073.
 - [24] V. Ziogas, J. High Energ. Phys. 09 (2015) 114.
 - [25] L. J. Henderson, R. A. Hennigar, R. B. Mann, A. R. H. Smith, and J. Zhang, Phys. Lett. B 809 (2020) 135732.
 - [26] L. de Souza Campos, and C. Dappiaggi, Phys. Lett. B 816 (2021) 136198.
 - [27] B. Koch, I. A. Reyes and A. Rincón, Class. Quantum Grav. 33 (2016) 225010.
 - [28] A. Rincón et al., Eur. Phys. J. C 77 (2017) 494.
 - [29] E. Contreras, A. Rincón, B. Koch and P. Bargueño, Int. J. Mod. Phys. D 27 (2017) 1850032.
 - [30] A. Rincón and G. Panotopoulos, Phys. Rev. D 97 (2018) 024027.
 - [31] E. Contreras, A. Rincón, B. Koch and P. Bargueño, Eur. Phys. J. C 78 (2018) 246 .
 - [32] A. Rincón and B. Koch, Eur. Phys. J. C 78 (2018) 1022.
 - [33] A. Rincón, E. Contreras, P. Bargueño, B. Koch and G. Panotopoulos, Eur. Phys. J. C 78 (2018) 641.
 - [34] A. Rincón, E. Contreras, P. Bargueño and B. Koch, Eur. Phys. J. Plus 134 (2019) 557.
 - [35] E. Contreras, A. Rincón, G. Panotopoulos, P. Bargueño and B. Koch, Phys. Rev. D 101 (2020) 064053.
 - [36] A. Rincón and J. R. Villanueva, Class. Quantum Grav. 37 (2020) 175003.
 - [37] M. Fathi, A. Rincón and J. R. Villanueva, Class. Quantum Grav. 37 (2020) 075004.
 - [38] F. Canales, B. Koch, C. Laporte and A. Rincón, J. Cosmol. Astropart. Phys. 01 (2020) 021.
 - [39] E. Contreras and P. Bargueño, Int. J. Mod. Phys. D 27 (2018) 1850101.
 - [40] A. Bonanno and M. Reuter, Phys. Rev. D 62 (2000) 043008.
 - [41] A. Bonanno and M. Reuter, Phys. Rev. D 65 (2002) 043508.

- [42] M. Reuter and H. Weyer, Phys. Rev. D 69 (2004) 104022.
- [43] C. Rubano and P. Scudellaro, Gen. Rel. Grav. 37 (2005) 521.
- [44] A. Bonanno and M. Reuter, Phys. Lett. B 527 (2002) 9.
- [45] L. H. Liu, T. Prokopec and A. A. Starobinsky, Phys. Rev. D 98 (2018) 043505.
- [46] M. Hindmarsh and I. D. Saltas, Phys. Rev. D 86 (2012) 064029.
- [47] A. Platania, Eur. Phys. J. C 79 (2019) 470.
- [48] R. Moti and A. Shojai, Int. J. Mod. Phys. A 35 (2020) 2050016.
- [49] B. Koch and F. Saueressig, Class. Quantum Grav. 31 (2014) 015006.
- [50] J. M. Pawłowski and D. Stock, Phys. Rev. D 98 (2018) 106008.
- [51] M. Cardenas, O. Fuentealba, and C. Martinez, Phys. Rev. D 90 (2014) 124072.
- [52] S. H. Hendi, B. Eslam Panah, and R. Saffari, Int. J. Mod. Phys. D 23 (2014) 1450088.
- [53] B. Gwak, and B. -H. Lee, Phys. Lett. B 755 (2016) 324.
- [54] S. Alsaleh, Int. J. Mod. Phys. A 32 (2017) 1750076.
- [55] K. S. Gupta, T. Jurić, and A. Samsarov, J. High Energ. Phys. 06 (2017) 107.
- [56] G. G. L. Nashed, and S. Capozziello, Int. J. Mod. Phys. A 33 (2018) 1850076.
- [57] X. -H. Ge, S. -J. Sin, Y. Tian, S. -F. Wu, and S. -Y. Wu, J. High Energ. Phys. 01 (2018) 068.
- [58] B. Eslam Panah, S. H. Hendi, S. Panahiyan, and M. Hassaine, Phys. Rev. D 98 (2018) 084006.
- [59] S. -T. Hong, Y. -W. Kim, and Y. -J. Park, Phys. Rev. D 99 (2019) 024047.
- [60] B. Mu, J. Tao, and P. Wang, Phys. Lett. B 800 (2020) 135098.
- [61] P. Cañate, D. Magos, and N. Breton, Phys. Rev. D 101 (2020) 064010.
- [62] T. Padmanabhan, Phys. Rep. 380 (2003) 235.
- [63] A. Silvestri, and M. Trodden, Rept. Prog. Phys. 72 (2009) 096901.
- [64] C. Armendariz-Picon, T. Damour, and V. Mukhanov, Phys. Lett. B 458 (1999) 209.
- [65] N. Bilic, G. B. Tupper, and R. D. Viollier, Phys. Lett. B 535 (2002) 17.
- [66] T. Multamaki, M. Manera, and E. Gaztanaga, Phys. Rev. D 69 (2004) 023004.
- [67] C. Brans, and R. H. Dicke, Phys. Rev. 124 (1961) 925.
- [68] D. Lovelock, J. Math. Phys. 12 (1971) 498.
- [69] A. A. Starobinsky, Phys. Lett. B 91 (1980) 99.
- [70] P. Brax, and C. van de Bruck, Class. Quantum Grav. 20 (2003) R201.
- [71] A. De Felice, and S. Tsujikawa, Living Rev. Rel. 13 (2010) 3.
- [72] T. P. Sotiriou and V. Faraoni, Rev. Mod. Phys. 82 (2010) 451.
- [73] K. Hinterbichler, Rev. Mod. Phys. 84 (2012) 671.
- [74] C. de Rham, Living Rev. Rel. 17 (2014) 7.
- [75] Y. Akrami, T. S. Koivisto, and M. Sandstad, J. High Energ. Phys. 03 (2013) 99.
- [76] Y. Akrami, S. F. Hassan, F. Kunnig, A. Schmidt-May, and A. R. Solomon, Phys. Lett. B 748 (2015) 37.
- [77] E. Babichev, L. Marzola, M. Raidal, A. Schmidt-May, F. Urban, H. Veerme, and M. von Strauss, Phys. Rev. D 94 (2016) 084055.
- [78] E. Babichev, L. Marzola, M. Raidal, A. Schmidt-May, F. Urban, H. Veerme, and M. von Strauss, J. Cosmol. Astropart. Phys. 09 (2016) 016.
- [79] S. Panpanich, and P. Burikham, Phys. Rev. D 98 (2018) 064008.
- [80] B. Eslam Panah, and H. L. Liu, Phys. Rev. D 99 (2019) 104074.
- [81] S. H. Hendi, G. H. Bordbar, B. Eslam Panah, and S. Panahiyan, J. Cosmol. Astropart. Phys. 07 (2017) 004.
- [82] J. Xu, L. M. Cao, and Y. P. Hu, Phys. Rev. D 91 (2015) 124033.
- [83] S. H. Hendi, R. B. Mann, S. Panahiyan, and B. Eslam Panah, Phys. Rev. D 95 (2017) 021501(R).
- [84] A. Dehghani, S. H. Hendi, and R. B. Mann, Phys. Rev. D 101 (2020) 084026.
- [85] B. Eslam Panah, S. H. Hendi, and Y. C. Ong, Phys. Dark Universe, 27 (2020) 100452.
- [86] M. -S. Hou, H. Xu, and Y. C. Ong, Eur. Phys. J. C 80 (2020) 1090.
- [87] C. de Rham, and G. Gabadadze, Phys. Rev. D 82 (2010) 044020.
- [88] C. de Rham, G. Gabadadze, and A. J. Tolley, Phys. Rev. Lett. 106 (2011) 231101.
- [89] H. van Dam, and M. Veltman, Nucl. Phys. B 22 (1970) 397.
- [90] V. Zakharov, JETP Lett. 12 (1970) 312.
- [91] D. G. Boulware, and S. Deser, Phys. Rev. D 6 (1972) 3368.
- [92] S. F. Hassan, and R. A. Rosen, Phys. Rev. Lett. 108 (2012) 041101.
- [93] M. Fierz, and W. Pauli, Proc. Roy. Soc. Lond. A 173 (1939) 211.
- [94] L. Alberte, and A. Khmelnitsky, Phys. Rev. D 91 (2015) 046006.
- [95] H. Zhang, and X-Z. Li, Phys. Rev. D 93 (2016) 124039.
- [96] T. Q. Do, Phys. Rev. D 93 (2016) 104003.
- [97] K. Koyama, G. Niz, and G. Tasinato, Phys. Rev. Lett. 107 (2011) 131101.
- [98] T. M. Nieuwenhuizen, Phys. Rev. D 84 (2011) 024038.
- [99] A. Gruzinov, and M. Mirbabayi, Phys. Rev. D 84 (2011) 124019.
- [100] L. Berezhiani, G. Chkareuli, C. de Rham, G. Gabadadze, and A. J. Tolley, Phys. Rev. D 85 (2012) 044024.
- [101] R. A. Rosen, J. High Energ. Phys. 10 (2017) 206.
- [102] D. Vegh, *Holography without translational symmetry*, [arXiv:1301.0537].
- [103] R. G. Cai, Y. P. Hu, Q. Y. Pan, and Y. L. Zhang, Phys. Rev. D 91 (2015) 024032.

- [104] S. H. Hendi, B. Eslam Panah, and S. Panahiyan, *J. High Energy Phys.* 11 (2015) 157.
- [105] S. H. Hendi, B. Eslam Panah, S. Panahiyan, H. Liu, and X.-H. Meng, *Phys. Lett. B* 781 (2018) 40.
- [106] C. H. Nam, *Gen. Rel. Grav.* 53 (2021) 30.
- [107] D. -C. Zou, Y. Liu, and R. Yue, *Eur. Phys. J. C* 77 (2017) 365.
- [108] S. H. Hendi, and M. Momennia, *J. High Energy Phys.* 10 (2019) 207.
- [109] M. Chabab, H. El Moumni, S. Iraoui, and K. Masmar, *Eur. Phys. J. Plus.* 135 (2020) 248.
- [110] M. Zhang, D. -C. Zou, and R. -H. Yue, *Advance. High Energy. Phys.* 2017 (2017) 3819246.
- [111] Y. Ma, Y. Zhang, L. Zhang, L. Wu, Y. Gao, S. Cao, and Y. Pan, *Eur. Phys. J. C* 81 (2021) 42.
- [112] Y. -B. Ma, S. -X. Zhang, Y. Wu, L. Ma, and S. Cao, *Commun. Theor. Phys.* 69 (2018) 544.
- [113] S. Chougule, S. Dey, B. Pourhassan, and M. Faizal, *Eur. Phys. J. C* 78 (2018) 685.
- [114] P. K. Yerra, and C. Bhamidipati, *Int. J. Mod. Phys. A* 35 (2020) 2050120.
- [115] Y. Ma, Y. Zhang, L. Zhang, L. Wu, Y. Huang, and Y. Pan, *Eur. Phys. J. C* 80 (2020) 213.
- [116] B. Wu, C. Wang, Z. -M. Xu, and W. -L. Yang, *Eur. Phys. J. C* 81 (2021) 626.
- [117] B. Eslam Panah, and S. H. Hendi, *Europhys. Lett.* 125 (2019) 60006.
- [118] M. Hassaine, and C. Martinez, *Phys. Rev. D* 75 (2007) 027502.
- [119] M. Hassaine, and C. Martinez, *Class. Quantum Grav.* 25 (2008) 195023.
- [120] H. Maeda, M. Hassaine, and C. Martinez, *Phys. Rev. D* 79 (2009) 044012.
- [121] S. H. Hendi, and B. Eslam Panah, *Phys. Lett. B* 684 (2010) 77.
- [122] J. Jing, Q. Pan, and S. Chen, *J. High Energ. Phys.* 11 (2011) 045.
- [123] D. Roychowdhury, *Phys. Lett. B* 718 (2013) 1089.
- [124] M. Zhang, Z. -Y. Yang, D. -C. Zou, W. Xu, and R. -H. Yue, *Gen. Rel. Grav.* 47 (2015) 14.
- [125] J. -X. Mo, G. -Q. Li, and X. -B. Xu, *Phys. Rev. D* 93 (2016) 084041.
- [126] H. -F. Li, X. -y. Guo, H. -H. Zhao, and R. Zhao, *Gen. Rel. Grav.* 49 (2017) 111.
- [127] S. H. Hendi, B. Eslam Panah, S. Panahiyan, and M. S. Talezadeh, *Eur. Phys. J. C* 77 (2017) 133.
- [128] A. Dehghani, and S. H. Hendi, *Phys. Rev. D* 104 (2021) 024025.
- [129] S. H. Hendi, B. Eslam Panah, and S. Panahiyan, *J. High Energ. Phys.* 05 (2016) 029.
- [130] S. W. Hawking, *Phys. Rev. Lett.* 26 (1971) 1344.
- [131] J. M. Bardeen, B. Carter, and S. W. Hawking, *Commun. Math. Phys.* 31 (1973) 161.
- [132] J. D. Beckenstein, *Phys. Rev. D* 7 (1973) 2333.
- [133] S. W. Hawking, C. J. Hunter, and D. N. Page, *Phys. Rev. D* 59 (1999) 044033.
- [134] B. Carter, *Phys. Rev.* 174 (1968) 1559.
- [135] Y. Decanini, A. Folacci, and B. Raffaelli, *Class. Quantum Grav.* 28 (2011) 175021.
- [136] H. Lu and H. D. Lyu, *Phys. Rev. D* 101 (2020) 044059.
- [137] V. Perlick, O. Y. Tsupko, and G. S. Bisnovaty-Kogan, *Phys. Rev. D* 92 (2015) 104031.
- [138] S. W. Wei, and Y. X. Liu, *J. Cosmol. Astropart. Phys.* 11 (2013) 063.
- [139] A. Belhaj, M. Benali, A. El Balali, H. El Moumni, and S. E. Ennadifi, *Class. Quantum Grav.* 37 (2020) 215004.
- [140] S. Chandrasekhar, " *The Mathematical Theory of Black Holes*", Oxford University Press, New York (1983).
- [141] S. Weinberg, " *Gravitation and Cosmology: Principles and Applications of the General Theory of Relativity*", (Wiley, New York, 1972).
- [142] P. Kocherlakota, and L. Rezzolla, *Phys. Rev. D* 102 (2020) 064058.
- [143] W. Javed, J. Abbas, and A. ovgun, *Ann. Phys.* 418 (2020) 168183.
- [144] A. Rincón and G. Panotopoulos, *Phys. Dark Univ.* 30 (2020) 100639.
- [145] K. Jusufi, *Phys. Rev. D* 101 (2020) 084055.
- [146] K. Jusufi, *Phys. Rev. D* 101 (2020) 124063.
- [147] R. A. Konoplya, and Z. Stuchlik, *Phys. Lett. B* 771 (2017) 597.
- [148] Y. Guo, and Y. G. Miao, *Phys. Rev. D* 102 (2020) 084057.
- [149] C. Lan, Y. G. Miao, and H. Yang, [arXiv: 2008.04609].
- [150] S. W. Wei, and Y. X. Liu, *Chin. Phys. C* 44 (2020) 115103.
- [151] V. Cardoso, A. S. Miranda, E. Berti, H. Witek and V. T. Zanchin, *Phys. Rev. D* 79 (2009) 064016.
- [152] R. A. Konoplya, *Phys. Rev. D* 66 (2002) 044009.
- [153] R. A. Konoplya, *Phys. Rev. D* 66 (2002) 084007.
- [154] V. Cardoso, R. Konoplya, and J. P. S. Lemos, *Phys. Rev. D* 68 (2003) 044024.
- [155] S. Fernando, *Gen. Rel. Grav.* 36 (2004) 71.
- [156] T. Regge, and J. A. Wheeler, *Phys. Rev.* 108 (1957) 1063.
- [157] F. J. Zerilli, *Phys. Rev. D* 2 (1970) 2141.
- [158] L. C. B. Crispino, A. Higuchi, E. S. Oliveira, and J. V. Rocha, *Phys. Rev. D* 87 (2013) 104034.
- [159] P. Kanti, T. Pappas, and N. Pappas, *Phys. Rev. D* 90 (2014) 124077.
- [160] T. Pappas, P. Kanti, and N. Pappas, *Phys. Rev. D* 94 (2016) 024035.
- [161] G. Panotopoulos, and A. Rincón, *Eur. Phys. J. Plus* 135 (2020) 33.
- [162] D. Mahdavian Yekta, and M. Shariat, *Class. Quantum Grav.* 36 (2019) 185005.
- [163] K. D. Kokkotas, and B. F. Schutz, *Phys. Rev. D* 37 (1988) 3378.
- [164] S. Fernando, and J. Correa, *Phys. Rev. D* 86 (2012) 064039.
- [165] <http://www.wolfram.com>
- [166] R. A. Konoplya and A. Zhidenko, *Phys. Rev. D* 81 (2010) 124036.